© 2014. Published by The Company of Biologists Ltd | Journal of Cell Science (2014) 127, 1672–1683 doi:10.1242/jcs.132316

RESEARCH ARTICLE

Paxillin controls endothelial cell migration and tumor angiogenesis by altering neuropilin 2 expression

Alexandra E. German[1,2], Tadanori Mammoto[2], Elisabeth Jiang[2], Donald E. Ingber[2,3,4,*] and Akiko Mammoto[2]

ABSTRACT

Although a number of growth factors and receptors are known to control tumor angiogenesis, relatively little is known about the mechanism by which these factors influence the directional endothelial cell migration required for cancer microvessel formation. Recently, it has been shown that the focal adhesion protein paxillin is required for directional migration of fibroblasts *in vitro*. Here, we show that paxillin knockdown enhances endothelial cell migration *in vitro* and stimulates angiogenesis during normal development and in response to tumor angiogenic factors *in vivo*. Paxillin produces these effects by decreasing expression of neuropilin 2 (NRP2). Moreover, soluble factors secreted by tumors that stimulate vascular ingrowth, including vascular endothelial growth factor (VEGF), also decrease endothelial cell expression of paxillin and NRP2, and overexpression of NRP2 reverses these effects. These results suggest that the VEGF–paxillin–NRP2 pathway could represent a new therapeutic target for cancer and other angiogenesis-related diseases.

KEY WORDS: Paxillin, Neuropilin 2, VEGF, Angiogenesis, Cancer, Capillary endothelial cell, Motility

INTRODUCTION

Capillary endothelial cell migration is mediated by dynamic remodeling of the actin cytoskeleton and linked focal adhesions that physically anchor cells to the underlying extracellular matrix (ECM). Focal adhesions also mediate mechano-chemical transduction through changes in the position and activity of many signal transducing molecules (e.g. small and large G proteins, protein kinases, inositol lipid kinases, ion channels, etc.) that physically associate with the cytoskeletal backbone of the focal adhesion (Wozniak et al., 2004). As a result, physical interactions between cells and ECM through integrins that locate in focal adhesions can influence the direction in which cells extend new lamellipodia and filopodia, and thereby control oriented cell movement (Brock and Ingber, 2005; Dike et al., 1999; Parker et al., 2002; Sero et al., 2011; Xia et al., 2008). Recently, we have shown that knockdown of the focal adhesion protein paxillin interferes with oriented lamellipodia extension and inhibits directional migration in fibroblasts by altering focal adhesion position (Sero et al., 2011). The present study was initiated to explore the possibility that paxillin might play a similar role in governing directional migration of capillary endothelial cells during tumor angiogenesis.

Paxillin is a multifunctional multidomain focal adhesion adaptor protein that is phosphorylated by Src and focal adhesion kinase (FAK) (Tachibana et al., 1995; Turner et al., 1990), and associates with many other focal adhesion proteins and signaling molecules (Brown and Turner, 2004; Deakin et al., 2012; Hagel et al., 2002; Sero et al., 2012; Turner et al., 1990). It can positively and negatively regulate cell migration depending on whether it is located at the leading edge (Nayal et al., 2006) or tail end (Nishiya et al., 2005) of the cell. Paxillin-knockout mice are embryonic lethal because of developmental defects in the mesoderm (Hagel et al., 2002), and paxillin knockdown causes defects in embryonic stem cell spreading (Wade et al., 2002) and enhances HeLa cell migration (Yano et al., 2004). Interestingly, paxillin mutations and changes in protein expression are also associated with alterations in the malignant progression of many tumors (Deakin et al., 2012), including breast (Madan et al., 2006; Short et al., 2007), lung (Jagadeeswaran et al., 2008; Mackinnon et al., 2011; Salgia et al., 1999), prostate (Sen et al., 2012), melanoma (Velasco-Velázquez et al., 2008) and colorectal cancer (Yang et al., 2010).

Directional capillary endothelial cell migration is an essential component of sprouting angiogenesis (Lamalice et al., 2007; Li et al., 2005). Because paxillin controls directional migration in fibroblasts (Plotnikov et al., 2012; Sero et al., 2011), it is possible that changes in paxillin expression or activity also influence capillary endothelial cell motility during tumorigenesis. In fact, in capillary endothelial cells, paxillin rapidly becomes phosphorylated in response to treatment with the tumor-associated vascular endothelial growth factor (VEGF), which is a potent motility factor (Abedi and Zachary, 1997). However, the mechanism by which paxillin might exert control over capillary endothelial cell migration and angiogenesis has never been explored in the context of tumor angiogenesis.

The ubiquitous angiogenic growth factor VEGF, and its receptors, have been implicated in control of directional capillary endothelial cell migration because they regulate expression or activities of signaling molecules that are central to migratory control, including Cdc42, Rho, Rho-associated protein kinase (ROCK), FAK, phosphatidylinositol-3 kinase (PI3K) and p38 MAPKs (Chung and Ferrara, 2011; Koch et al., 2011; Lohela et al., 2009). VEGF acts through VEGF receptor 2 (VEGFR2) (Chung and Ferrara, 2011; Koch et al., 2011; Lamalice et al., 2007; Lohela et al., 2009) and through its non-kinase receptor neuropilin 2 (NRP2) (Geretti et al., 2008; Gluzman-Poltorak et al., 2000; Neufeld et al., 2002), which is expressed in endothelial cells (Gluzman-Poltorak et al., 2000; Takashima et al., 2002) as well as neuronal cells where it plays a central role in axon guidance. NRP2

[1]Harvard-MIT Division of Health Sciences and Technology, MIT, Cambridge, MA 02139, USA. [2]Vascular Biology Program, Departments of Pathology & Surgery, Boston Children's Hospital and Harvard Medical School, Boston, MA 02115, USA. [3]Wyss Institute for Biologically Inspired Engineering at Harvard University, Boston, MA 02115, USA. [4]Harvard School of Engineering and Applied Sciences, Cambridge, MA 02139, USA.

*Author for correspondence (don.ingber@wyss.harvard.edu)

Received 1 April 2013; Accepted 22 January 2014

Journal of Cell Science

Journal of Cell Science (2014) 127, 1672–1683 doi:10.1242/jcs.132316

deficiency suppresses lymphatic vessel development (Yuan et al., 2002), embryonic angiogenesis (Takashima et al., 2002) and retinal neovascularization in the presence of ischemia (Shen et al., 2004). Importantly, it has also been suggested that NRP2 plays a role in tumor angiogenesis because it is required for semaphorin 3F (Sema3F)-dependent chemorepulsion of capillary endothelial cells, which appears to be disrupted during tumor progression (Bielenberg et al., 2004).

Here, we show that paxillin knockdown increases capillary endothelial cell migration and invasiveness, and thereby enhances microvessel ingrowth, by suppressing NRP2 expression *in vitro* and *in vivo*. In addition, our findings show that soluble tumor-derived factors produce similar effects through decreasing paxillin expression in capillary endothelial cells. The paxillin–NRP2 axis might therefore represent a new target for therapeutic modulation or normalization of the tumor vasculature.

RESULTS

Paxillin controls endothelial cell migration

Our recent finding that paxillin regulates directional cell migration in fibroblasts (Sero et al., 2011) led us to examine whether paxillin also controls oriented migration of endothelial cells, which is required for capillary network formation during angiogenesis. Human umbilical vein endothelial cell (HUVEC) migration was analyzed in Transwell migration chambers using EBM2 supplemented with bFGF (also known as FGF2), VEGF, IGF, EGF and 5% serum. Treatment with two distinct small interfering RNA (siRNA) sequences against paxillin resulted in knockdown of paxillin expression by ~90% as confirmed by immunoblotting and qRT-PCR (Fig. 1A,B). Paxillin knockdown cells exhibited an ~2-fold increase in migration after 24 hours when compared with control cells transfected with scrambled siRNA (Fig. 1C). When the Transwell chambers were coated with Matrigel to create a 3D ECM invasion assay (Sero et al., 2011), the paxillin knockdown cells again displayed an ~2-fold increase in the average distance they invaded into gel relative to control cells (Fig. 1D,E), which is consistent with increases in directional cell migration produced by knocking out paxillin in mouse embryonic fibroblasts (Sero et al., 2011). These data show that paxillin expression might be required for control of the normal processes of directional endothelial cell migration and invasion that underlie capillary network formation.

We then explored whether paxillin knockdown also alters capillary endothelial cell migration and invasion *in vivo*. Matrigel plugs were pre-cast in poly-dimethylsiloxane (PDMS) polymer molds and implanted subcutaneously in a mouse. Then, paxillin or control siRNA (10 µg) was injected into the plug after 3 days, and vascular ingrowth was analyzed 4 days later, as described previously (Mammoto et al., 2009) (supplementary material Fig. S1A). Treatment with paxillin siRNA decreased paxillin expression in infiltrating CD31+ cells by 60% as measured by immunofluorescence staining (Fig. 2A,B) and by ~50% in all cells when analyzed by qRT-PCR (Fig. 2C). Interestingly, suppression of paxillin expression resulted in ~1.5-fold increase in the number of CD31+ capillary endothelial cells that invaded into the Matrigel plugs (Fig. 2D,E). Quantification of the number of capillary endothelial cells at increasing depths through the gel revealed that there were 2- to 8-fold increases in the number of capillary endothelial cells throughout the depth of gels containing paxillin siRNA compared to control gels (Fig. 2F). This increased ingrowth of capillary microvessels was confirmed by perfusing the entire mouse vasculature with fluoresceinated-concanavalin A (ConA) via injection into the retro-orbital vein just prior to harvesting the implants, and generating 3D reconstructions (Fig. 2G; supplementary material Fig. S1B). Thus, knocking down paxillin expression not only increased capillary endothelial

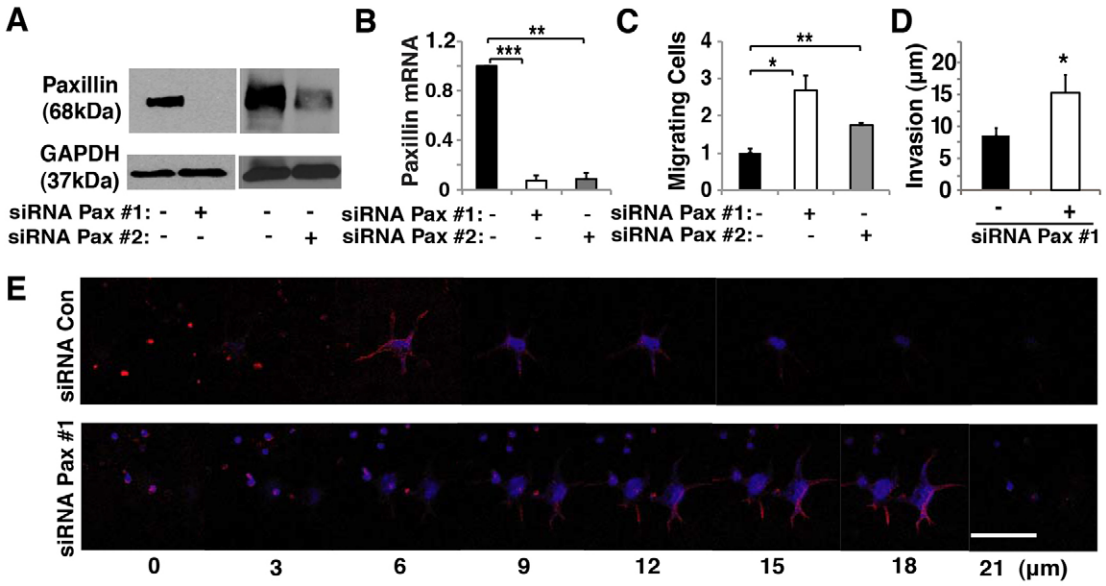

Fig. 1. Paxillin controls endothelial cell migration *in vitro*. (A) Immunoblots showing paxillin and GAPDH protein levels in HUVECs transfected with control (lanes negative for the paxillin siRNA) or paxillin-targeted siRNAs (Pax #1, Pax #2). (B) Graph showing mRNA level of paxillin in HUVECs treated with control or paxillin siRNA. (C) Graph showing the number of migrating HUVECs transfected with control or paxillin siRNA normalized to the control-siRNA-transfected cells in Transwell migration assay. The migratory stimulus is 5% serum EGM2. (D) Graph showing the distance of invasion of HUVECs transfected with control or paxillin siRNA in a Transwell invasion assay. The migratory stimulus is 5% serum EGM2. In B–D, black bars indicate cells transfected with control siRNA. Data are means±s.e.m. *$P<0.05$, **$P<0.01$; ***$P<0.001$. (E) Confocal micrographs showing HUVEC invasion into Matrigel transfected with control (Con) or paxillin siRNA with 5% EGM2 as chemoattractant. Scale bar: 50 µm.

Journal of Cell Science (2014) 127, 1672–1683 doi:10.1242/jcs.132316

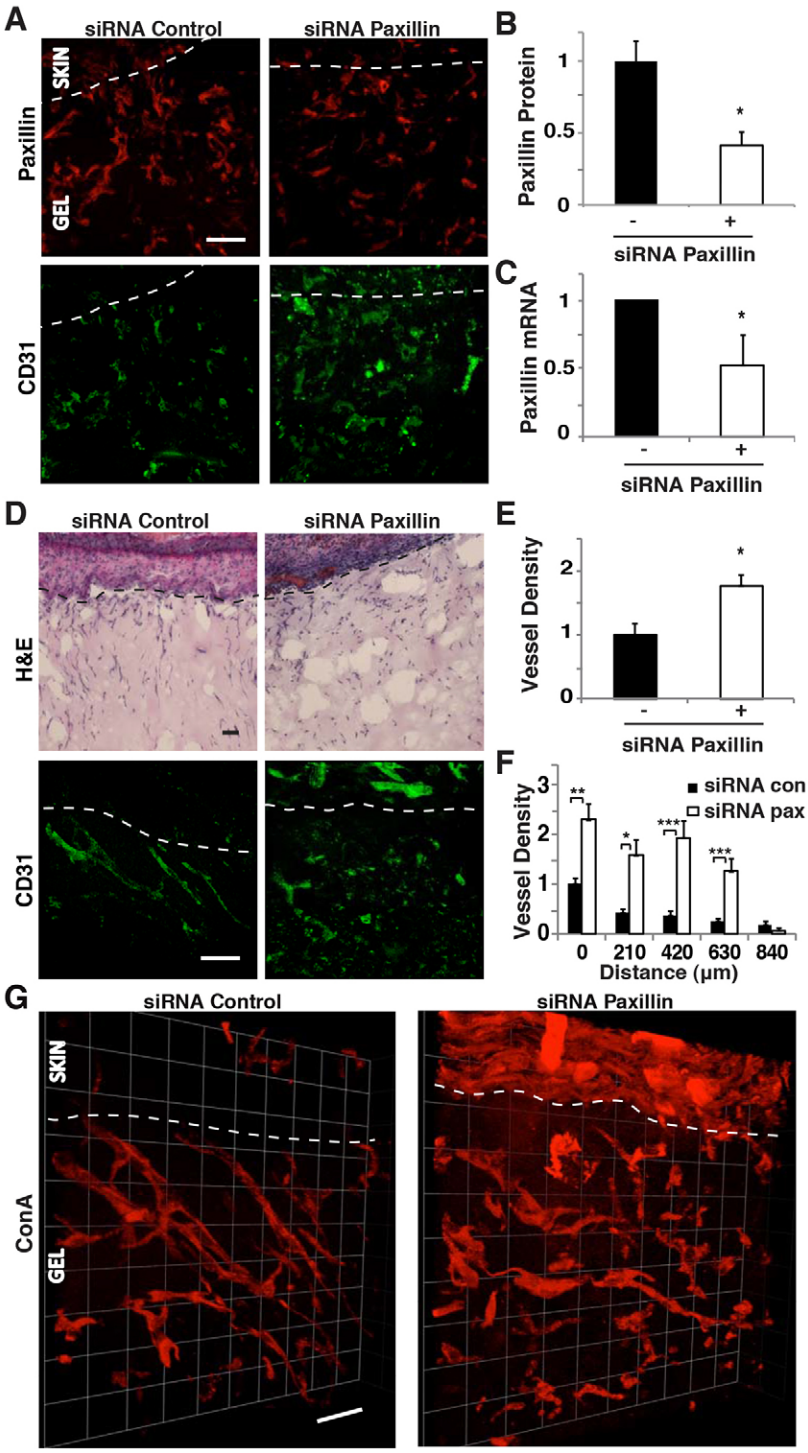

Fig. 2. Paxillin controls endothelial cell migration *in vivo*. (A) Confocal micrographs showing paxillin expression (top) and CD31 expression (bottom) in the Matrigel implanted subcutaneously on the back of C57BL/6 mice treated with control or paxillin siRNA. The region of skin is shown above the dotted line, and Matrigel with invading cells is below the dotted line. (B) Graph showing paxillin protein levels, quantified by using immunohistochemical image analysis where paxillin colocalized to CD31+ cells was measured in three random 50×50-μm fields per gel (n=5). (C) Graph showing mRNA level of paxillin in the infiltrated cells in the implanted Matrigel (n=8). (D) H&E-stained micrographs showing host-cell migration from C57BL/6 mouse skin into implanted Matrigel treated with control or paxillin siRNA (top). Confocal micrographs showing CD31-stained endothelial cells in the Matrigel treated with control or paxillin siRNA (bottom). (E) Quantification of endothelial cell density in the implanted Matrigel with control or paxillin siRNA from immunohistochemical CD31 image analysis (n=7). In B, C and E, black bars indicate mice treated with control siRNA. (F) Graph showing migration distance of CD31-stained endothelial cells from the skin into Matrigel implant treated with control or paxillin siRNA (n=6). (G) 3D reconstructed confocal micrographs of a Matrigel implant treated with control or paxillin siRNA perfused with fluorescein-ConA. Scale bars: 50 μm. Data are means±s.e.m. *P<0.05; **P<0.01; ***P<0.001. See also supplementary material Fig. S1.

cell ingrowth, it also stimulated formation of new functional microvessels *in vivo*. The total number of cells (e.g. immune cells, fibroblasts and capillary endothelial cells) migrating into the Matrigel plug did not vary significantly between control and paxillin siRNA-treated implants (Fig. 2D; supplementary material Fig. S1C,D). Suppression of paxillin also did not alter the number of CD45+ immune cells that invaded the gels (supplementary material Fig. S1E); however, it significantly decreased the number of fibroblasts that invaded the gel (supplementary material Fig. S1F). Therefore, it appears that paxillin suppression has different effects on cell migration *in vivo* depending on the cell type.

Paxillin controls retinal angiogenesis *in vivo*

We then examined whether paxillin is also important for control of normal developmental angiogenesis *in vivo* by analyzing the effects of paxillin knockdown during mouse neonatal retinal angiogenesis. This is a relevant model system because directional cell migration is required for new microvessel formation in the growing retina (Gerhardt et al., 2003; Wacker and Gerhardt,

Journal of Cell Science (2014) 127, 1672–1683 doi:10.1242/jcs.132316

2011). Paxillin siRNA (0.5 μg) was injected directly into the vitreous humor of a postnatal day 4 (P4) mouse eye, the eye was harvested 2 days later and the vessels were visualized by staining with fluorescent isolectin. Knockdown of paxillin resulted in increased formation of sprouts throughout the forming vascular network (Fig. 3A,B). We also studied the retinal vascular network at P8 (by this point most of the vessels reach the edge of the retina). Knockdown of paxillin resulted in increased tortuous microvessel formation as indicated by a 1.5-fold increase in vessel density compared to control-siRNA-treated eyes (Fig. 3C,D). Thus, suppression of paxillin expression appears to result in enhanced migration *in vitro*, as well as increased microvascular ingrowth *in vivo* during normal vessel development.

Paxillin controls angiogenesis by altering NRP2 expression

VEGF is one of the most ubiquitous angiogenic factors and it plays a key role in controlling capillary endothelial cell migration (Chung and Ferrara, 2011; Koch et al., 2011; Lohela et al., 2009). The cell surface VEGF receptor NRP2 controls endothelial cell survival and migration in response to VEGF (Favier et al., 2006; Takashima et al., 2002). Therefore, we examined whether paxillin might control endothelial cell migration by altering NRP2 expression. siRNA-mediated knockdown of paxillin resulted in a 50% decrease in NRP2 expression at both protein and mRNA levels in cultured HUVECs (Fig. 4A–C). To determine whether these effects are specific for paxillin, we explored whether other key focal adhesion proteins (vinculin and zyxin) also affect NRP2 expression and endothelial cell motility. However, knockdown of vinculin or zyxin did not alter NRP2 expression nor change endothelial cell migration in a Transwell migration assay (supplementary material Fig. S2A–C). Moreover, when NRP2 was knocked down using siRNA (supplementary material Fig. S2D–F), HUVEC migration increased by 1.5-fold (Fig. 4D), and invasion into Matrigel doubled (Fig. 4E,F), much as it did when paxillin was knocked down in these cells (Fig. 1C–E). Importantly, overexpression of NRP2, which increases NRP2 mRNA and protein levels in capillary endothelial cells (supplementary material Fig. S2D–F), was able to prevent the increase of HUVEC migration and invasion in paxillin knockdown cells (Fig. 4D–F). Thus, NRP2 appears to mediate the effects of paxillin on endothelial cell motility and invasion *in vitro*.

We have previously shown that overexpression of a paxillin N-terminal (paxN) truncation mutant in paxillin-knockout mouse embryonic fibroblasts results in a significant increase in their invasive behavior, whereas expression of a C-terminal (paxC) truncation mutant has the opposite effect (Sero et al., 2011). To

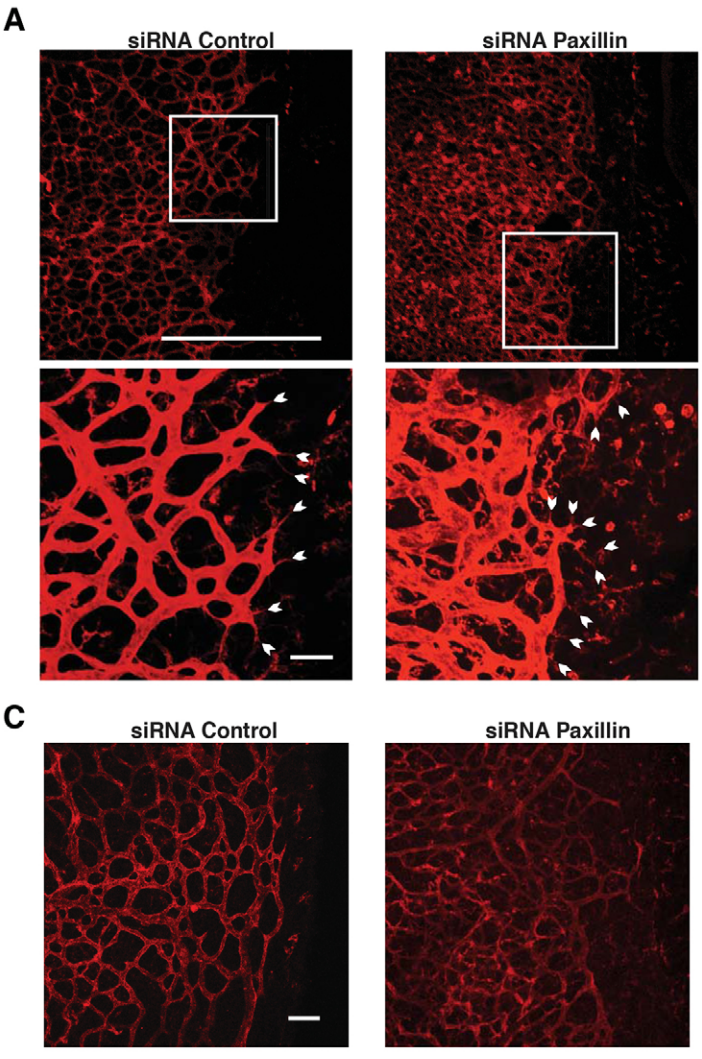

Fig. 3. Paxillin controls formation of sprouts during mouse neonatal retinal angiogenesis. (A) Confocal images of isolectin-stained retina from P6 neonatal mouse 2 days post intravitreous injection of control or paxillin siRNA. Scale bars: 0.5 mm (top micrograph); 50 μm (bottom micrograph). White arrowheads indicate sprouts and sprout orientation. (B) Normalized average number of sprouts per 400×200-μm retinal area with control (black bars) or paxillin siRNA (white bars) (n=3). (C) Confocal images of isolectin-stained retina from P10 neonatal mice 2 days post intravitreous injection of control or paxillin siRNA. Scale bar: 0.1 mm. (D) Graph showing the vessel density of peripheral region of retina treated with paxillin siRNA normalized with that from control-siRNA-treated retina (n=6). Data are means±s.e.m. *P<0.05; **P<0.01.

Journal of Cell Science (2014) 127, 1672–1683 doi:10.1242/jcs.132316

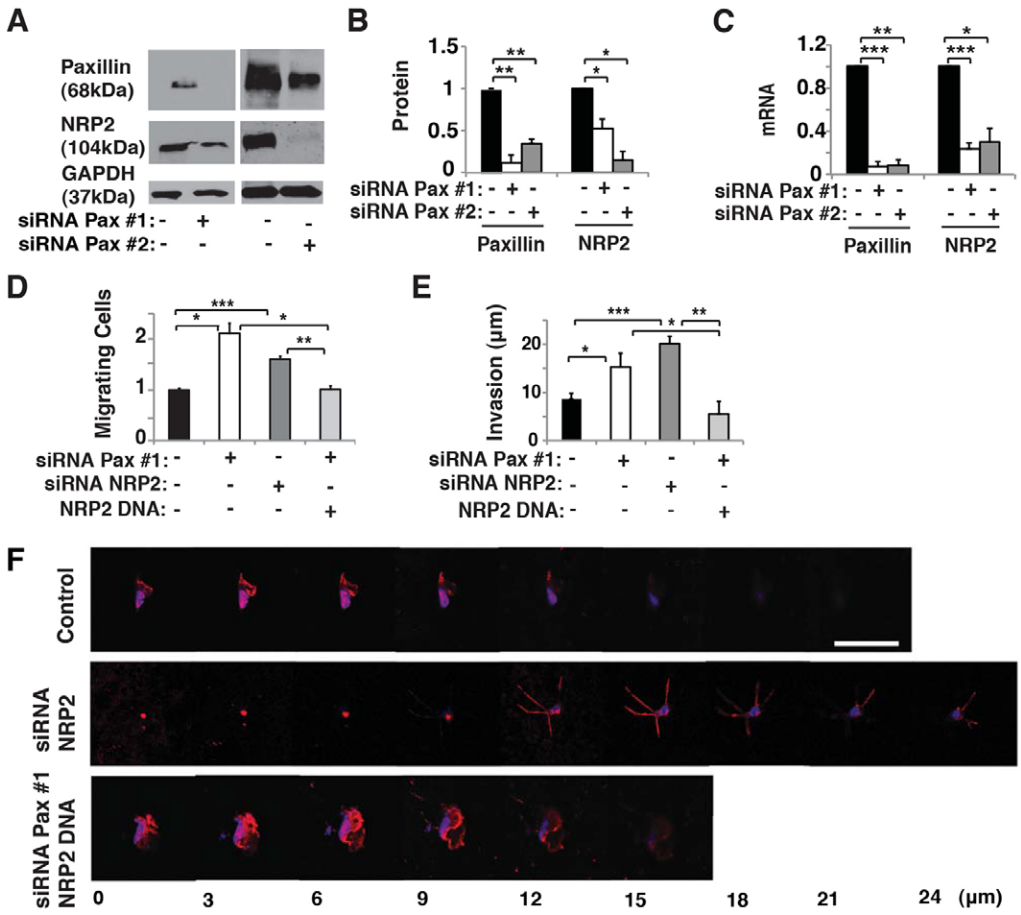

Fig. 4. Paxillin controls NRP2 expression and endothelial migration *in vitro*. (A) Immunoblots of paxillin, NRP2 and GAPDH in HUVECs treated with control (lanes negative for the paxillin siRNA) or paxillin siRNA. (B) Graph showing quantification of protein levels of paxillin and NRP2 in HUVECs treated with control or paxillin siRNA. (C) Graph showing mRNA levels of paxillin and NRP2 in HUVECs treated with control or paxillin siRNA. (D) Graph showing number of migrating HUVECs treated with paxillin siRNA, NRP2 siRNA, or paxillin siRNA plus NRP2 DNA normalized by control-siRNA-transfected cells in Transwell migration assay. (E) Graph showing invasion distance of HUVECs treated with paxillin siRNA, NRP2 siRNA, or paxillin siRNA plus NRP2 DNA in a Transwell invasion assay. The migratory stimulus is 5% serum EGM2. Data are represented as mean±s.e.m. *$P<0.05$; **$P<0.01$; ***$P<0.001$. In B–E, black bars indicate cells treated with control siRNA. (F) Confocal micrographs showing HUVEC invasion in a Transwell invasion assay with 5% EGM2 as chemoattractant in combination with NRP2 siRNA or paxillin siRNA plus NRP2 DNA. Scale bar: 50 µm. See also supplementary material Fig. S2.

further analyze the molecular mechanism through which paxillin controls endothelial cell migration, we examined whether overexpression of paxillin truncation mutants could control endothelial cell migration. When paxN was overexpressed in paxillin-knockdown HUVECs *in vitro* (supplementary material Fig. S2G), we detected a 20% increase in cell migration relative to paxillin knockdown cells alone (supplementary material Fig. S2H). In contrast, overexpression of paxC (supplementary material Fig. S2G) did not produce any significant change in migratory behavior (supplementary material Fig. S2H). Importantly, this migration-stimulating effect of overexpressing paxN in paxillin knockdown HUVECs was accompanied by a decrease in NRP2 protein levels, whereas paxC overexpression had no effect on NRP2 protein expression (supplementary material Fig. S2G). Therefore, the N-terminal portion of paxillin appears to mediate its ability to promote migration in endothelial cells by suppressing NRP2 expression.

To determine the physiological relevance of these effects, we measured the expression of NRP2 in capillary endothelial cells that infiltrated Matrigel plug implants in the *in vivo* Matrigel capillary invasion assay when we knocked down paxillin expression. NRP2 expression decreased by 40% in capillary endothelial cells, as measured by image analysis, when paxillin siRNA was injected subcutaneously (Fig. 5A,B), and a similar decrease in NRP2 mRNA level was measured by analyzing total mRNA in gel implants using qRT-PCR (Fig. 5C). We then injected NRP2-specific siRNA subcutaneously, and found that it produced ~60% knockdown of NRP2 protein and mRNA levels (supplementary material Fig. S3A–C). Direct knockdown of NRP2 did not alter the total number of cells (e.g. immune cells, fibroblasts and capillary endothelial cells) migrating into the Matrigel plug (Fig. 5D; supplementary material Fig. S3D); however, it specifically produced an increase in endothelial cell migration resulting in significantly enhanced capillary ingrowth into the gel (Fig. 5D,E). This resulted in the appearance of a higher number of capillary endothelial cells at increasing distances into the gel relative to control gels (Fig. 5F), hence mimicking the results we observed by knocking down paxillin (Fig. 2F). In addition, NRP2 knockdown increased the number of functional vessels perfused by fluorescent ConA and visualized in 3D reconstructions (Fig. 5G; supplementary material Fig. S3E). These results indicate that paxillin controls NRP2 expression both *in vitro* and *in vivo*, and that siRNA-mediated knockdown of NRP2 enhances endothelial cell migration and microvascular invasion, resulting in a phenotype nearly identical to that produced by inhibiting paxillin expression.

Although NRP2 acts as a VEGF receptor, VEGFR2 is the key receptor VEGF utilizes to stimulate angiogenesis, and it also plays a key role in controlling capillary endothelial cell migration (Chung and Ferrara, 2011; Koch et al., 2011; Lamalice et al., 2007; Lohela et al., 2009). We therefore explored whether paxillin controls capillary endothelial cell migration by altering VEGFR2 expression. These studies revealed, however, that paxillin knockdown did not significantly change VEGFR2 expression in capillary endothelial cells that infiltrated into the implanted Matrigel plugs *in vivo* (supplementary material Fig.

Journal of Cell Science (2014) 127, 1672–1683 doi:10.1242/jcs.132316

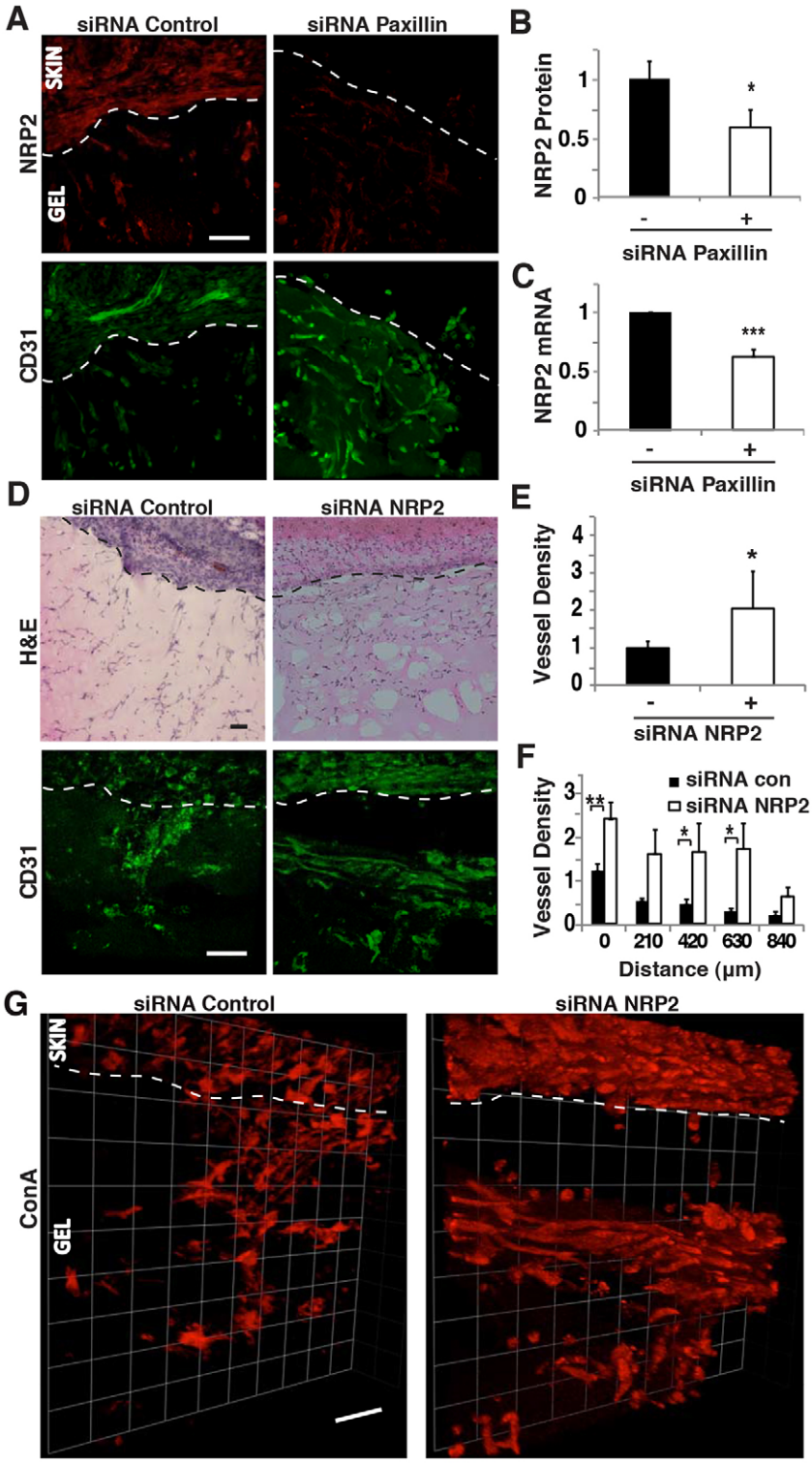

Fig. 5. NRP2 knockdown enhances endothelial cell migration *in vivo*. (A) Confocal micrographs showing NRP2 expression (top) and CD31-stained endothelial cells (bottom) in Matrigel implanted subcutaneously on the back of a C57BL/6 mouse treated with control or paxillin siRNA. (B) Graph showing NRP2 protein levels quantified by immunohistochemical image analysis where NRP2 colocalized to CD31+ cells as measured in three random 50×50-μm fields per gel (n=5). (C) Graph showing mRNA level of NRP2 in the infiltrated cells in the implanted Matrigel (n=8). (D) H&E-stained micrographs showing host-cell migration from C57BL/6 mouse skin into implanted Matrigel treated with control or NRP2 siRNA (top). Confocal micrographs showing CD31-stained endothelial cells migrated in the Matrigel implant with control or NRP2 siRNA (bottom). (E) Quantification of CD31+ endothelial cell migration into Matrigel implant treated with control (black bars) or NRP2 (white bars) siRNA as measured in three random 50×50-μm fields per gel (n=4). In B, C and E, black bars indicate mice treated with control siRNA. (F) Graph showing migration distance of CD31-positive endothelial cells into Matrigel implant treated with control or NRP2 siRNA (n=4). (G) 3D reconstructed confocal micrographs of Matrigel implant treated with control or NRP2 siRNA perfused with fluorescein-ConA. Data are represented as mean±s.e.m. *P<0.05; **P<0.01; ***P<0.001. Scale bars: 50 μm. See also supplementary material Fig. S3.

S3F–H). Thus, paxillin appears to exert its angiogenesis-modulating effects by selectively altering NRP2 expression.

Paxillin mediates tumor-induced angiogenesis

Formation of well-organized microvessels is necessary for normal organ development and deregulation of this process contributes to cancer progression, as well as to development of tumor resistance to cancer therapies (Carmeliet and Jain, 2011; Chung and Ferrara, 2011). We therefore set out to examine whether paxillin is also involved in control of tumor-induced angiogenesis. To do this, we implanted a Matrigel plug subcutaneously within one chamber of a two-chamber PDMS device that contained Lewis lung carcinoma (LLC) cells in the second chamber, separated from the Matrigel by a porous filter membrane (supplementary material Fig. S4A). LLC cells are unable to escape (data not shown), but the soluble factors they produce diffuse through

Journal of Cell Science (2014) 127, 1672–1683 doi:10.1242/jcs.132316

pores of the membrane and act as chemoattractants to stimulate migration of host cells into the Matrigel. LLC cells are known to secrete VEGF, as well as multiple other soluble growth factors (Satchi-Fainaro et al., 2005).

We found that the presence of LLC-derived angiogenic factors decreased cellular expression of paxillin in fluorescent ConA-staining cells by 40% and 90%, as demonstrated by computerized image analysis of immunohistochemically stained sections (Fig. 6A,B) and qRT-PCR of extracted Matrigel (Fig. 6C), respectively. The presence of LLC-derived factors in the second chamber also resulted in a significant increase in total number of migrating cells, in capillary endothelial cell migration and in the number of capillary endothelial cells that appeared at increasing depths into the gel compared to single-chamber implants (supplementary material Fig. S4B–E). As expected, tumor-derived factors also increased the total number of

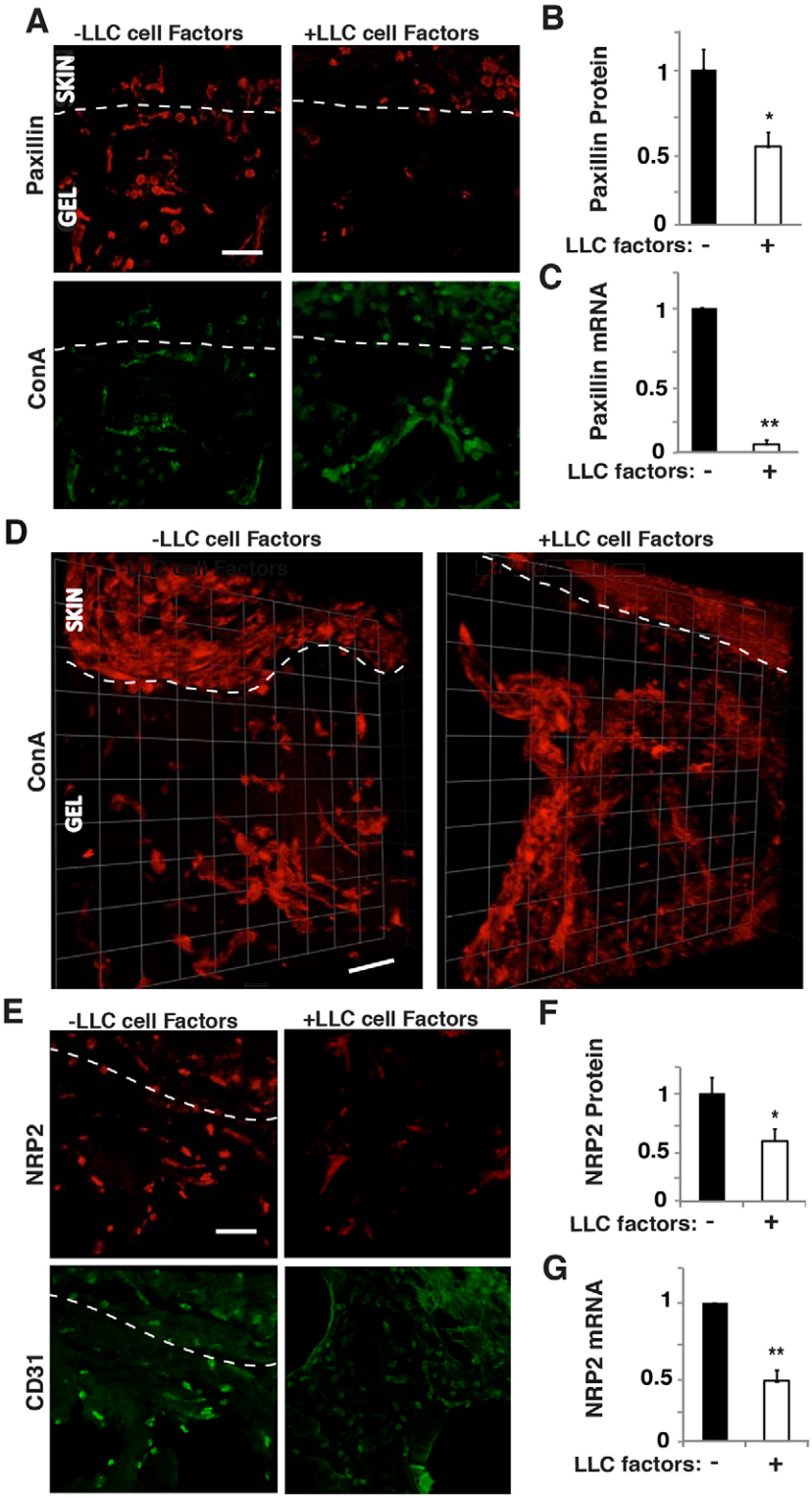

Fig. 6. Paxillin and NRP2 mediate endothelial cell migration and invasion induced by tumor factors *in vivo*. (A) Confocal micrographs showing paxillin expression (top) and ConA-stained vessels (bottom) in infiltrated cells in the Matrigel implant with or without LLC factors. (B) Graph showing paxillin protein levels quantified by immunohistochemical image analysis where paxillin colocalized to fluorescent ConA-staining cells as measured in three random 50×50-μm fields per gel (n=5). (C) Graph showing mRNA level of paxillin in the infiltrated cells in the implanted Matrigel (n=6). (D) 3D reconstructed confocal micrographs of Matrigel implant with or without LLC factors perfused with fluorescein-ConA. (E) Confocal micrographs showing NRP2 expression (top) and CD31-stained endothelial cells (bottom) migrated into the implanted Matrigel with or without LLC factors. (F) Graph showing NRP2 protein levels quantified by immunohistochemical image analysis of NRP2 colocalized with CD31+ cells as measured in three random 50×50-μm fields per gel (n=4). (G) Graph showing mRNA level of NRP2 in the infiltrated cells in the implanted Matrigel (n=8). Data are represented as mean±s.e.m. *P<0.05; **P<0.01. Scale bars: 50 μm. See also supplementary material Fig. S4.

Journal of Cell Science (2014) 127, 1672–1683 doi:10.1242/jcs.132316

functional vessels as indicated by perfusing with fluorescent ConA and carrying out 3D reconstructions (Fig. 6D; supplementary material Fig. S4F). Taken together, these results indicate that soluble angiogenic factors produced by the LLC tumor both suppress paxillin expression and greatly increase capillary endothelial cell migration and microvascular invasion *in vivo*.

The soluble factors secreted by LLC cells that decreased paxillin expression in capillary endothelial cells by 40% (Fig. 6A,B) also reduced capillary endothelial cell expression of NRP2 by 30–50%, when analyzed by immunohistochemistry (Fig. 6E,F) or measuring total NRP2 mRNA levels in the Matrigel plug implants (Fig. 6G). Thus, it appears that the endogenous expression of paxillin is decreased by the presence of tumor factors and this, in turn, suppresses NRP2 expression *in vivo*, just as it does *in vitro*. To test this hypothesis, we examined whether tumor factors promote angiogenesis *in vitro* by altering paxillin expression, and thereby modulating NRP2 levels. Indeed, conditioned medium collected from LLC cell cultures decreased expression of both paxillin protein and mRNA levels (Fig. 7A–C) by ~70% and ~50%, respectively in cultured HUVECs, much as we observed in our *in vivo* studies (Fig. 6A–C). Moreover, NRP2

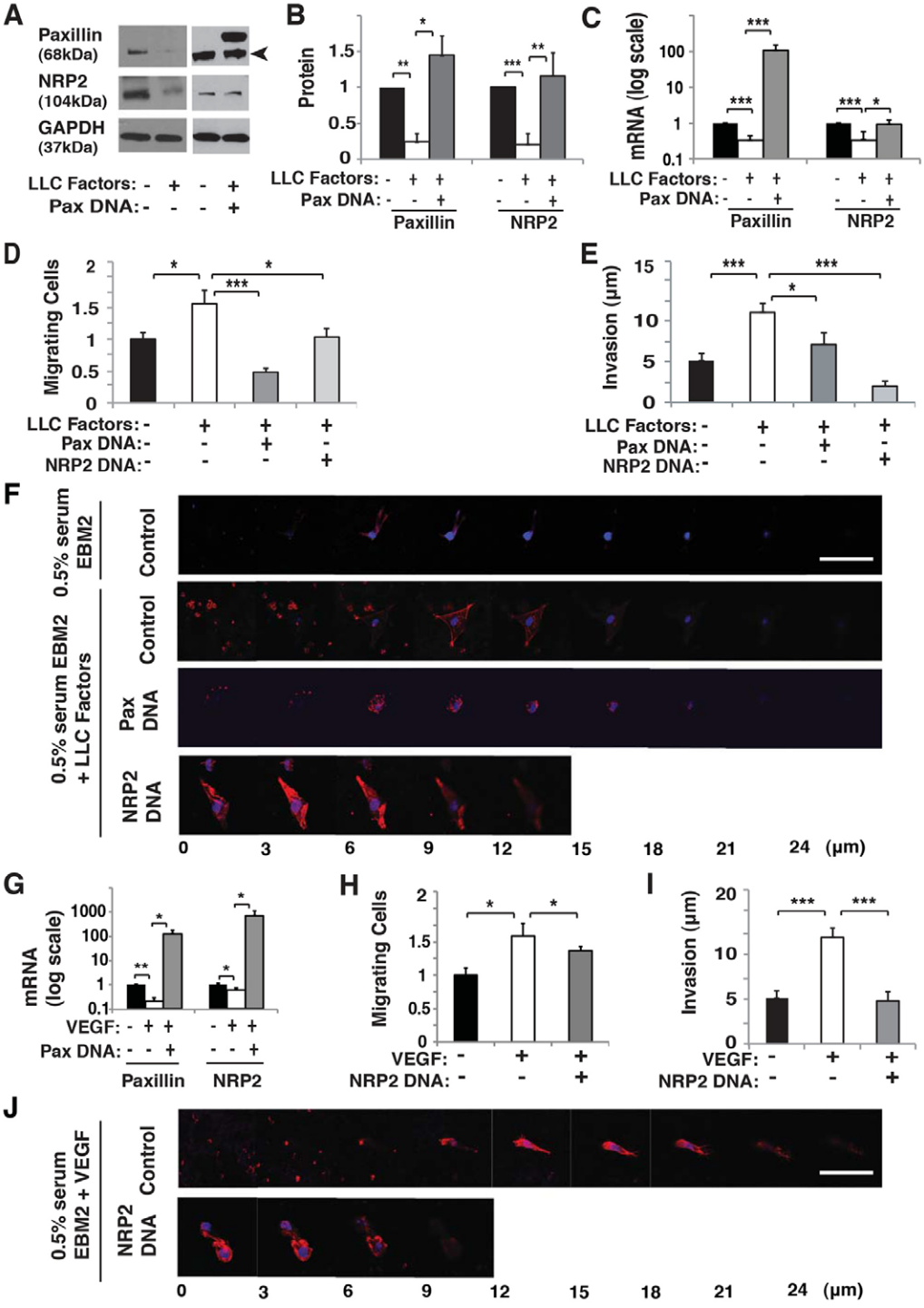

Fig. 7. LLC factors and VEGF control HUVEC migration and invasion through paxillin–NRP2 signaling. (A) Immunoblots showing paxillin, NRP2 and GAPDH protein levels in HUVECs treated with 0.5% serum EBM2 with or without LLC factors, or in combination with paxillin DNA. The arrowhead indicates paxillin. (B) Quantification of immunoblotting in A showing protein levels of paxillin and NRP2. (C) Graph showing mRNA level of paxillin and NRP2 in HUVECs treated with 0.5% serum EBM2 with or without LLC factors, or in combination with paxillin DNA. (D) Graph showing number of HUVECs migrating towards 0.5% serum EBM2 with or without LLC factors in combination with paxillin DNA or NRP2 DNA treatment in a Transwell migration assay. (E) Graph showing invasion distance of HUVECs to 0.5% serum EBM2 with or without LLC factors in combination with paxillin DNA or NRP2 DNA treatment in a Transwell migration assay. (F) Confocal micrographs showing HUVEC invasion in a Transwell invasion assay with 0.5% serum EBM2 or paxillin DNA or NRP2 DNA with LLC-conditioned 0.5% serum EBM2. (G) Graph showing paxillin and NRP2 mRNA levels from HUVECs in 0.5% serum EBM2 with or without VEGF (30 ng/ml), or in combination with paxillin DNA. (H) Graph showing number of HUVECs migrating towards 0.5% serum EBM2 with or without VEGF in combination with NRP2 DNA in a Transwell migration assay. (I) Graph showing invasion distance of HUVECs to 0.5% serum EBM2 with or without VEGF in combination with NRP2 DNA in a Transwell migration assay. (J) Confocal micrographs showing HUVEC invasion in a Transwell invasion assay with or without NRP2 DNA with VEGF-conditioned 0.5% serum EBM2. Data are represented as mean±s.e.m. *$P<0.05$; **$P<0.01$; ***$P<0.001$. Scale bars: 50 μm.

Journal of Cell Science (2014) 127, 1672–1683 doi:10.1242/jcs.132316

expression decreased by at least 50% when the cultured HUVECs were stimulated with LLC factors that also decrease paxillin expression (Fig. 7A–C), whereas overexpression of paxillin restored normal NRP2 levels (Fig. 7A–C). Thus, again, NRP2 appears to be downstream of paxillin in this signaling pathway.

When we examined the effects of LLC-derived factors on HUVEC migration and invasion *in vitro*, the tumor factors increased the number of migrating cells that invaded into the Matrigel plugs by 1.5-fold and 2-fold, respectively (Fig. 7D–F). Furthermore, when we overexpressed paxillin in LLC factor-treated cells, cell migration and invasion were restored to control levels (Fig. 7D–F). Similar normalization of capillary endothelial cell migration and ECM invasion was also obtained by overexpressing NRP2 (Fig. 7D–F).

VEGF decreases paxillin expression and NRP2 expression

As VEGF is a major angiogenic chemoattractant produced by LLC cells (Satchi-Fainaro et al., 2005) and NRP2 is a VEGF receptor, we explored whether VEGF could be responsible for the effects of tumor-derived factors on paxillin and NRP2 expression that we observed. VEGF alone decreased paxillin expression by ~80% when measured by qRT-PCR (Fig. 7G), in addition to suppressing expression of NRP2 mRNA (Fig. 7G), much as we observed in our studies with LLC-derived factors. Moreover, paxillin overexpression in combination with VEGF was able to reverse the suppression of NRP2 mRNA levels (Fig. 7G). Importantly, VEGF-induced increases in HUVEC migration (Fig. 7H) and invasion (Fig. 7I,J) also were suppressed by overexpressing NRP2 (Fig. 7H–J). Taken together, these experiments show that soluble tumor-derived factors, such as VEGF, stimulate microvessel ingrowth, at least in part, by decreasing endogenous expression of paxillin, which in turn leads to suppression of NRP2, and an associated increase in migration and invasion of endothelial cells.

DISCUSSION

Paxillin governs proper spatial positioning of focal adhesions and lamellipodia in fibroblasts that are required for directional migration, and its absence results in enhanced (albeit disordered) cell migration (Sero et al., 2011). Although the role of paxillin in cell motility has been explored extensively, its function during angiogenesis remained unclear. Here, we show that knockdown of paxillin using siRNA transfection decreases expression of the capillary endothelial cell guidance molecule, and angiogenic VEGF receptor, NRP2 (Bielenberg et al., 2004; Gluzman-Poltorak et al., 2000; Takashima et al., 2002). Moreover, this results in increases in endothelial cell migration *in vitro*, as well as enhanced capillary sprouting in the developing retina and increased microvascular invasion in Matrigel implants *in vivo*. Importantly, we also discovered that the expression of paxillin is decreased by tumor-derived soluble factors including VEGF, which in turn suppresses NRP2 expression and enhances microvessel formation. Given that both normal retinal vascular development and tumor neovascularization are mediated by VEGF (Chung and Ferrara, 2011; Lohela et al., 2009), these observations suggest that VEGF–paxillin–NRP2 signaling plays a central role in both normal and tumor angiogenesis. Thus, modifiers of this new signaling pathway might offer an alternative strategy for treatment of cancer and other angiogenesis-related diseases.

It remains unclear how paxillin controls NRP2 expression. Our studies suggest that the paxillin N-terminus controls NRP2 expression and thereby, stimulates endothelial cell migration. In fact, the paxillin N-terminus interacts with a number of signaling molecules that regulate transcription and migration (Deakin and Turner, 2008; Sero et al., 2012). For example, p190RhoGAP (also known as ARHGAP35) has been shown to control the activity of paxillin phosphorylated at Y31 and Y118 (Tsubouchi et al., 2002), and p190RhoGAP also controls VEGFR2 expression through a balance of the transcription factors GATA2 and TFII-I (Mammoto et al., 2009). Interestingly, NRP2 has a GATA2-binding site in its promoter region, and thus, the paxillin N-terminus could control NRP2 expression by interacting with signaling molecules that associate with p190RhoGAP and GATA2. The VEGF-phosphorylated transcription factor ELK1 (Murata et al., 2000) also can bind to the NRP2 promoter region. ELK1 has been reported to form a complex with nuclear paxillin to regulate cell functions (Sen et al., 2012), and so paxillin could control NRP2 transcriptional activity through ELK1 in capillary endothelial cells. It is as yet unknown whether paxillin controls the expression of receptors for other angiogenic factors besides NRP2. Although p190RhoGAP regulates VEGFR2 expression (Mammoto et al., 2009), paxillin did not significantly modulate VEGFR2 expression in our Matrigel plugs *in vivo*. Finally, it is possible that paxillin controls endothelial cell migration both upstream and downstream of NRP2 because even though paxillin interacts with p190RhoGAP and controls NRP2 expression, p190RhoGAP has been shown to act downstream of NRP2 to inhibit cell motility (Shimizu et al., 2008).

Although we previously reported that paxillin knockdown promotes fibroblast migration *in vitro* (Sero et al., 2011), in our *in vivo* Matrigel implants, paxillin knockdown decreased fibroblast migration. This might be because of differences in ECM or soluble factors *in vivo*, or be due to paracrine effects of other cell types that infiltrate the Matrigel *in vivo* (e.g. endothelial or immune cells). Although paxillin knockdown decreased fibroblast infiltration into the Matrigel implants, it significantly increased migration of endothelial cells. It is possible that this endothelial response we observed *in vivo* could be a secondary effect of decreased fibroblast migration. However, fibroblasts produce ECM components and secrete soluble factors that can both inhibit endothelial cell migration as well as promote it (Chung and Ferrara, 2011; Kut et al., 2007). Thus, given our *in vitro* findings demonstrating that paxillin knockdown directly promotes endothelial cell migration *in vitro* by changing NRP2 expression, and we see similar changes in NRP *in vivo*, we believe that a similar mechanism is responsible for the vascular ingrowth we observed in the Matrigel implants.

Our studies revealed that soluble tumor factors decrease paxillin expression and thereby enhance capillary endothelial cell migration that drives angiogenesis and microvascular invasion. Mechanical forces also contribute to control of capillary cell growth, migration and fate determination (Mammoto and Ingber, 2009; Mammoto et al., 2012), and changes in mechanical forces elicited by altering ECM stiffness can regulate angiogenesis through p190RhoGAP (Mammoto et al., 2009). Given that paxillin mediates force-dependent control of cell behaviors (Sawada and Sheetz, 2002; Zaidel-Bar et al., 2007), including directional cell motility (Plotnikov et al., 2012; Polacheck et al., 2014; Sero et al., 2011), cell-derived mechanical forces might also contribute to the control of angiogenesis through paxillin.

Paxillin knockdown and a subsequent decrease in NRP2 expression increased endothelial cell migration *in vitro* and *in vivo* in the present study; however, the mechanism by which

paxillin knockdown results in enhanced microvascular network formation remains unclear. We have previously shown that paxillin is not required for focal adhesion formation or total cell migration in fibroblasts, but that it is required for tension sensing, proper localization of both focal adhesions and lamellipodia, and directional migration (Sero et al., 2011). Thus, suppression of paxillin and NRP2, both of which are required for directional cell motility, appear to result in an inability of endothelial cells to properly localize focal adhesion remodeling and motile processes, resulting in haphazard and enhanced migration as observed in the tumor vasculature. The suppression of NRP2 expression also might contribute to these effects by decreasing binding of its ligand Semaphorin 3F (Sema3F), which is a chemorepulsive cytokine that normally suppresses motile process formation and endothelial cell movement (Bielenberg et al., 2004; Bielenberg et al., 2006; Carmeliet, 2005; Geretti et al., 2008). Although decreased expression of NRP2 also would decrease binding of its ligand VEGF, this angiogenic factor can still stimulate endothelial cells through its other receptor, VEGFR2. This hypothetical mechanism conflicts, however, with the finding that NRP2 knockdown can inhibit VEGF-induced migration of endothelial cells *in vitro* (Favier et al., 2006). However, this inhibition might be due to differences in experimental settings, for example, we used whole serum or LLC tumor cell extract as a stimulant, whereas the other studies used only VEGF. In addition to VEGF and Sema3F, other molecules that can modulate cell migration, such as bFGF, PDGF, HGF and TGF-β1 (Wild et al., 2012) have been shown to bind NRP2, and LLC cells have been shown to produce both chemoattractive and repulsive factors (O'Reilly et al., 1994). Thus, the balance of attractive and repulsive cues might control the degree and direction of cell migration, as well as microvascular network formation, through their common receptor NRP2.

Interestingly, our finding that soluble tumor-derived factors decreased paxillin and NRP2 expression *in vitro* and *in vivo* is consistent with past reports that have shown that paxillin is decreased in lung, breast and colorectal tumors, among others (Deakin et al., 2012; Salgia et al., 1999; Yang et al., 2010). This seems to be controversial because paxillin expression has also been reported to be elevated in lung, prostate, breast, cervical and other tumors (Deakin et al., 2012; Jagadeeswaran et al., 2008; Mackinnon et al., 2011; Salgia et al., 1999; Sen et al., 2012). These conflicting results might be because these studies did not address the specific expression of paxillin in tumor endothelial cells because different cell components of cancers (e.g. parenchymal tumor cells, stroma fibroblasts, immune cells, endothelial cells) can respond in different ways to the same tumor factors. Alternatively, there might be differences in growth factor secretion and/or requirement among these different tumor types.

Also pertinent to our studies are past findings which have shown that modulation of paxillin has potential clinical implications for cancer. For example, inhibition of paxillin phosphorylation by the sialytransferase inhibitor Lith-O-Asp or other small molecules suppress lung tumor progression and metastasis (Chen et al., 2011; Huang et al., 2012), as well as breast cancer progression (Golubovskaya et al., 2008), *in vivo*. Interestingly, these molecules affect phosphorylation activity in the N-terminal region of paxillin, and we have shown here and in a previous study that the expression of the N-terminal alone substantially increases migration when transfected into paxillin knockdown cells, where N-terminus and C-terminus of paxillin have been shown to have complementary but opposite effects on cell migration and invasion (Sero et al., 2011). Thus, modulation of the N- or C-terminus of paxillin could be responsible for the mitigated migration and metastasis seen in past studies. In any case, these observations suggest that modifying the expression and activity (i.e. phosphorylation) of paxillin in endothelial cells could be a promising strategy for cancer therapy.

In summary, we have demonstrated that paxillin controls directional migration of endothelial cells, as well as microvessel invasion *in vitro* and *in vivo*, and that its expression is regulated by soluble tumor factors through VEGF–NRP2 signaling. Given that paxillin expression is altered in various cancers that are characterized by enhanced angiogenesis, development of modifiers of paxillin expression and/or activity could represent a new avenue for therapeutic development in cancer and other angiogenesis-related diseases.

MATERIALS AND METHODS

Materials

Anti-paxillin monoclonal antibody was from Abcam (Cambridge, MA, USA), anti-NRP2 monoclonal antibody was from Santa Cruz Biotechnology (Santa Cruz, CA, USA), anti-CD31 monoclonal antibody was from BD Biosciences (San Diego, CA, USA), anti-SMA monoclonal antibody was from Epitomics (Burlingame, CA, USA), anti-vinculin monoclonal antibody was from Sigma (St Louis, MI, USA), anti-zyxin monoclonal antibody was from Abcam (Cambridge, MA, USA), anti-GFP antibody was from BioVision (Milpitas, CA, USA), anti-GAPDH antibody was from Millipore (Billericka, MA, USA), anti-VEGFR2 antibody was from Cell Signaling, and Alexa-Fluor-488-conjugated phalliodin was from Invitrogen. Recombinant human (rh)VEGF was from R&D Systems (Minneapolis, MN, USA).

Cell culture

HUVECs (Lonza, Walkersville MD, USA) were cultured in EBM2 (Lonza, Walkersville MD, USA) medium with 5% fetal bovine serum (FBS) and growth factors (VEGF, bFGF, PDGF) (Lonza, Walkersville MD, USA). LLC cells were cultured in Dulbecco's modified Eagle's medium (DMEM) with 10% FBS (Gibco, Invitrogen, Carlsbad, CA, USA). LLC-conditioned medium was generated from confluent LLC monolayers after 24 hours of culture in 0.5% serum EBM2. To stimulate cells with VEGF, we added rhVEGF to 0.5% serum EBM2 to obtain a concentration of 30 ng/ml. Knockdown of paxillin, vinculin and zyxin (Ambion, Austin, TX, USA) and NRP2 (Sigma, St. Louis, MI, USA) was performed with siRNA (supplementary material Table S1) transfected into cells using the siLentFect transfection reagent (Bio-Rad, Hercules, CA, USA). An siRNA duplex with irrelevant sequence served as a control (Ambion, Austin TX, USA). Overexpression of human paxillin (pSport-Paxillin, Open Biosystems) and human NRP2 (a gift from Michael Klagsbrun, Boston Children's Hospital, MA; Shimizu et al., 2008) were performed using Superfect transfection reagent (Qiagen, Valencia, CA, USA). Transfection with vehicle alone served as control. The effects of knockdown and overexpression were confirmed via qRT-PCR and western blotting at 48–72 hours after transfection. GFP-tagged human paxillin N-terminus (paxN) and human paxillin C-terminus (paxC) truncation mutants (Sero et al., 2011) were transfected into siRNA-based paxillin knocked down HUVECs. We ensured that the siRNA did not also knockdown the transfected paxN and paxC mutants by using two sequences of siRNA against paxillin acting in the two different termini (e.g. paxillin siRNA #1 with target sequence in the paxillin C terminus was used in combination with paxN transfection, and paxillin siRNA #2 with target sequence in the N-terminus was used with paxC transfection).

Molecular biology assays

RNA was purified using an RNeasy mini kit (Qiagen, Valencia, CA, USA). qRT-PCR was performed with iScript cDNA synthesis kit (Bio-Rad, Hercules, CA, USA) and iTaq Sybr Green Supermix (Bio-Rad, Hercules, CA, USA) using a CFX96 real-time PCR machine (Bio-Rad,

Hercules, CA, USA). β2 microglobulin or cyclophilin controlled for cDNA content. Primers for paxillin, zyxin, vinculin, NRP2 and VEGFR2 are described in supplementary material Table S2.

Cell biological methods

Transwell migration assays

A total of 6×10^5 HUVECs per ml in 0.5% EBM2 were cultured on a 1% gelatin (Sigma, St. Louis, MI, USA)-coated membrane (Corning) and placed in a well with a chemoattractant (5% serum EGM2, 0.5% serum EBM2 plus 30 ng/ml rhVEGF or 0.5% serum EBM2 plus LLC-conditioned medium at a 2:1 ratio) (Mammoto et al., 2009). Cells were stained with Giemsa solution (Sigma, St. Louis, MI, USA) 24 hours later and counted in four random fields in three or more independent experiments.

Transwell invasion assay

Matrigel was added to an 8-μm-pore Transwell insert (Corning). A total of 3×10^6 cells/ml in 5% EGM2 were cultured on the underside of an inverted insert for 2 hours, the insert was then placed in a well with chemoattractant (described above) and incubated for 24 hours (Sero et al., 2011). Fixed inserts were incubated with Matrigel immunofluorescence wash buffer (130 mM NaCl, 7 mM Na_2HPO_4, 3.5 mM NaH_2PO_4, 0.1% BSA, 0.2% Triton X-100, 0.05% Tween-20) and stained with Alexa-Fluor-488-conjugated phalliodin (Invitrogen, Carlsbad, CA, USA) and DAPI. Images were taken at 25℃ on a Leica TCS SP2 confocal laser scanning microscope at excitations of 405 nm and 594 nm with a 63× 1.40 NA oil objective using Leica confocal software 2.61 at 3-μm *z*-plane slices through the depth of the Matrigel. Image analysis was performed with ImageJ software. Immunocytochemical image analysis was performed by measuring the depth of the center of the cell.

In vivo Matrigel plug assay

All animal studies were reviewed and approved by the Animal Care and Use Committee at Boston Children's Hospital. Matrigel plugs were cast in 7×7×2-mm PDMS molds and implanted subcutaneously on the back of a C57BL/6 mouse (Mammoto et al., 2009) (supplementary material Fig. S1A). Cancer model implants had an adjacent mold with 1×10^6 LLC cells encased in 0.22-μm membranes (Whatman, Clifton, NJ, USA) (supplementary material Fig. S4A). 10 μg of siRNA paxillin, siRNA NRP2 or scramble control siRNA was injected locally at day 3 after implantation. Fluorescein-ConA (Vector Laboratories, Burlingame, CA, USA) was injected into the retro-orbital vein prior to harvesting at day 7. Implants were fixed, frozen, sectioned and stained with hematoxylin and eosin (H&E), anti-CD31, paxillin, NRP2, VEGFR2 and DAPI antibodies. H&E stained images were taken on a Nikon Eclipse E600 microscope, fluorescent images were taken at 25℃ on a Leica TCS SP2 confocal laser scanning microscope at excitation wavelengths of 405 nm, 488 nm and/or 594 nm with a 63× 1.40 NA or 40× 1.25 NA oil objective and Leica confocal software version 2.61. Immunohistochemical vessel density analysis was performed by quantifying the expression of CD31 and fluorescent ConA per three different 50×50-μm areas of Matrigel for more than three independent implants using ImageJ software. In brief, projected *z*-stack images of 30-μm thick gel sections stained with CD31 or perfused with fluorescent ConA were binarized and positively staining areas were quantified using ImageJ software. NRP2, VEGFR2 and paxillin expression was measured when colocalized with CD31+ or fluorescent ConA-staining cells for three 50×50-μm areas of Matrigel for more than three implants. Invasion distance was measured by taking images through the depth of the gel (beginning at the skin line and moving away from the skin) and measuring the distance of CD31+ cells using ImageJ software. Migration of immune cells and fibroblasts was quantified by counting the number of CD45+ cells and smooth muscle actin (SMA+ and CD31−) cells, respectively, in 50×50-μm areas of Matrigel for more than three independent implants using ImageJ software. Stacks of 5–20 immunohistochemical images (1–3 μm between images) were complied to form 3D images using Volocity 4.4 Software (Improvision).

In vivo retinal vessel formation

0.5 μg of paxillin siRNA was injected intravitreally into one eye of a P4 or P8 neonatal C57BL/6 mouse and control siRNA was injected into the other eye. The eyeball was harvested 2 days later. Flat mounted, fixed tissues were stained with fluorescein-conjugated isolectin and imaged (Mammoto et al., 2009) at 25℃ using a Leica TCS SP2 confocal laser scanning microscope at an excitation wavelength of 594 nm with a 5× air or 20× 0.70 NA oil objective, and Leica confocal software 2.61. Stacks of 5–20 images were complied with Volocity 4.4 Software as above. Vessel density was quantified using Adobe Photoshop as described above. Isolectin-staining sprouts within 100 μm of the retina edge were counted using ImageJ.

Statistical Analysis

All experiments were repeated independently three or more times and data are represented as mean±s.e.m. Statistical analyses to assess the difference between control and treatment groups were performed with MATLAB R2012b software (Mathworks, Natick, MA, USA) using the unpaired Student's *t*-test.

Acknowledgements

We would like to thank Amanda Jiang and Tracy Tat for technical help. We also would like to thank Michael Klagsbrun for providing the NRP2 plasmid.

Competing interests

The authors declare no competing interests.

Author contributions

A.E.G., D.E.I. and A.M. conceived and designed the experiments. A.E.G., T.M., E.J. and A.M. performed the experiments. A.E.G., T.M., D.E.I. and A.M. analyzed the data. A.E.G., T.M. and A.M. contributed reagents, materials and/or analysis tools. A.E.G., A.M. and D.E.I. wrote the paper.

Funding

This work was supported by funds from National Science Foundation (NSF) Graduate Student Research Fellowship Program (to A.E.G.), the National Institutes of Health (NIH) [grant number CA45548 to D.E.I.]; the US Department of Defense [grant number BC074986 to D.E.I.]; the American Heart Association (to A.M.); and the American Brain Tumor Association (to A.M.). Deposited in PMC for release after 12 months.

Supplementary material

Supplementary material available online at
http://jcs.biologists.org/lookup/suppl/doi:10.1242/jcs.132316/-/DC1

References

Abedi, H. and Zachary, I. (1997). Vascular endothelial growth factor stimulates tyrosine phosphorylation and recruitment to new focal adhesions of focal adhesion kinase and paxillin in endothelial cells. *J. Biol. Chem.* **272**, 15442-15451.

Bielenberg, D. R., Hida, Y., Shimizu, A., Kaipainen, A., Kreuter, M., Kim, C. C. and Klagsbrun, M. (2004). Semaphorin 3F, a chemorepulsant for endothelial cells, induces a poorly vascularized, encapsulated, nonmetastatic tumor phenotype. *J. Clin. Invest.* **114**, 1260-1271.

Bielenberg, D. R., Pettaway, C. A., Takashima, S. and Klagsbrun, M. (2006). Neuropilins in neoplasms: expression, regulation, and function. *Exp. Cell Res.* **312**, 584-593.

Brock, A. L. and Ingber, D. E. (2005). Control of the direction of lamellipodia extension through changes in the balance between Rac and Rho activities. *Mol. Cell. Biomech.* **2**, 135-143.

Brown, M. C. and Turner, C. E. (2004). Paxillin: adapting to change. *Physiol. Rev.* **84**, 1315-1339.

Carmeliet, P. (2005). Angiogenesis in life, disease and medicine. *Nature* **438**, 932-936.

Carmeliet, P. and Jain, R. K. (2011). Molecular mechanisms and clinical applications of angiogenesis. *Nature* **473**, 298-307.

Chen, J. Y., Tang, Y. A., Huang, S. M., Juan, H. F., Wu, L. W., Sun, Y. C., Wang, S. C., Wu, K. W., Balraj, G., Chang, T. T. et al. (2011). A novel sialyltransferase inhibitor suppresses FAK/paxillin signaling and cancer angiogenesis and metastasis pathways. *Cancer Res.* **71**, 473-483.

Chung, A. S. and Ferrara, N. (2011). Developmental and pathological angiogenesis. *Annu. Rev. Cell Dev. Biol.* **27**, 563-584.

Deakin, N. O. and Turner, C. E. (2008). Paxillin comes of age. *J. Cell Sci.* **121**, 2435-2444.

Deakin, N. O., Pignatelli, J. and Turner, C. E. (2012). Diverse roles for the paxillin family of proteins in cancer. *Genes Cancer* **3**, 362-370.

Dike, L. E., Chen, C. S., Mrksich, M., Tien, J., Whitesides, G. M. and Ingber, D. E. (1999). Geometric control of switching between growth, apoptosis, and differentiation during angiogenesis using micropatterned substrates. *In Vitro Cell. Dev. Biol. Anim.* **35**, 441-448.

Favier, B., Alam, A., Barron, P., Bonnin, J., Laboudie, P., Fons, P., Mandron, M., Herault, J.-P., Neufeld, G., Savi, P. et al. (2006). Neuropilin-2 interacts with VEGFR-2 and VEGFR-3 and promotes human endothelial cell survival and migration. *Blood* **108**, 1243-1250.

Geretti, E., Shimizu, A. and Klagsbrun, M. (2008). Neuropilin structure governs VEGF and semaphorin binding and regulates angiogenesis. *Angiogenesis* **11**, 31-39.

Gerhardt, H., Golding, M., Fruttiger, M., Ruhrberg, C., Lundkvist, A., Abramsson, A., Jeltsch, M., Mitchell, C., Alitalo, K., Shima, D. et al. (2003). VEGF guides angiogenic sprouting utilizing endothelial tip cell filopodia. *J. Cell Biol.* **161**, 1163-1177.

Gluzman-Poltorak, Z., Cohen, T., Herzog, Y. and Neufeld, G. (2000). Neuropilin-2 is a receptor for the vascular endothelial growth factor (VEGF) forms VEGF-145 and VEGF-165 [corrected]. *J. Biol. Chem.* **275**, 18040-18045.

Golubovskaya, V. M., Nyberg, C., Zheng, M., Kweh, F., Magis, A., Ostrov, D. and Cance, W. G. (2008). A small molecule inhibitor, 1,2,4,5-benzenetetraamine tetrahydrochloride, targeting the y397 site of focal adhesion kinase decreases tumor growth. *J. Med. Chem.* **51**, 7405-7416.

Hagel, M., George, E. L., Kim, A., Tamimi, R., Opitz, S. L., Turner, C. E., Imamoto, A. and Thomas, S. M. (2002). The adaptor protein paxillin is essential for normal development in the mouse and is a critical transducer of fibronectin signaling. *Mol. Cell. Biol.* **22**, 901-915.

Huang, S. M., Hsu, P. C., Chen, M. Y., Li, W. S., More, S. V., Lu, K. T. and Wang, Y. C. (2012). The novel indole compound SK228 induces apoptosis and FAK/Paxillin disruption in tumor cell lines and inhibits growth of tumor graft in the nude mouse. *Int. J. Cancer* **131**, 722-732.

Jagadeeswaran, R., Surawska, H., Krishnaswamy, S., Janamanchi, V., Mackinnon, A. C., Seiwert, T. Y., Loganathan, S., Kanteti, R., Reichman, T., Nallasura, V. et al. (2008). Paxillin is a target for somatic mutations in lung cancer: implications for cell growth and invasion. *Cancer Res.* **68**, 132-142.

Koch, S., Tugues, S., Li, X., Gualandi, L. and Claesson-Welsh, L. (2011). Signal transduction by vascular endothelial growth factor receptors. *Biochem. J.* **437**, 169-183.

Kut, C., Mac Gabhann, F. and Popel, A. S. (2007). Where is VEGF in the body? A meta-analysis of VEGF distribution in cancer. *Br. J. Cancer* **97**, 978-985.

Lamalice, L., Le Boeuf, F. and Huot, J. (2007). Endothelial cell migration during angiogenesis. *Circ. Res.* **100**, 782-794.

Li, S., Guan, J. L. and Chien, S. (2005). Biochemistry and biomechanics of cell motility. *Annu. Rev. Biomed. Eng.* **7**, 105-150.

Lohela, M., Bry, M., Tammela, T. and Alitalo, K. (2009). VEGFs and receptors involved in angiogenesis versus lymphangiogenesis. *Curr. Opin. Cell Biol.* **21**, 154-165.

Mackinnon, A. C., Tretiakova, M., Henderson, L., Mehta, R. G., Yan, B. C., Joseph, L., Krausz, T., Husain, A. N., Reid, M. E. and Salgia, R. (2011). Paxillin expression and amplification in early lung lesions of high-risk patients, lung adenocarcinoma and metastatic disease. *J. Clin. Pathol.* **64**, 16-24.

Madan, R., Smolkin, M. B., Cocker, R., Fayyad, R. and Oktay, M. H. (2006). Focal adhesion proteins as markers of malignant transformation and prognostic indicators in breast carcinoma. *Hum. Pathol.* **37**, 9-15.

Mammoto, A. and Ingber, D. E. (2009). Cytoskeletal control of growth and cell fate switching. *Curr. Opin. Cell Biol.* **21**, 864-870.

Mammoto, A., Connor, K. M., Mammoto, T., Yung, C. W., Huh, D., Aderman, C. M., Mostoslavsky, G., Smith, L. E. and Ingber, D. E. (2009). A mechanosensitive transcriptional mechanism that controls angiogenesis. *Nature* **457**, 1103-1108.

Mammoto, A., Mammoto, T. and Ingber, D. E. (2012). Mechanosensitive mechanisms in transcriptional regulation. *J. Cell Sci.* **125**, 3061-3073.

Murata, M., Kador, P. F. and Sato, S. (2000). Vascular endothelial growth factor (VEGF) enhances the expression of receptors and activates mitogen-activated protein (MAP) kinase of dog retinal capillary endothelial cells. *J. Ocul. Pharmacol. Ther.* **16**, 383-391.

Nayal, A., Webb, D. J., Brown, C. M., Schaefer, E. M., Vicente-Manzanares, M. and Horwitz, A. R. (2006). Paxillin phosphorylation at Ser273 localizes a GIT1-PIX-PAK complex and regulates adhesion and protrusion dynamics. *J. Cell Biol.* **173**, 587-589.

Neufeld, G., Kessler, O. and Herzog, Y. (2002). The interaction of Neuropilin-1 and Neuropilin-2 with tyrosine-kinase receptors for VEGF. *Adv. Exp. Med. Biol.* **515**, 81-90.

Nishiya, N., Kiosses, W. B., Han, J. and Ginsberg, M. H. (2005). An alpha4 integrin-paxillin-Arf-GAP complex restricts Rac activation to the leading edge of migrating cells. *Nat. Cell Biol.* **7**, 343-352.

O'Reilly, M. S., Holmgren, L., Shing, Y., Chen, C., Rosenthal, R. A., Moses, M., Lane, W. S., Cao, Y., Sage, E. H. and Folkman, J. (1994). Angiostatin: a novel angiogenesis inhibitor that mediates the suppression of metastases by a Lewis lung carcinoma. *Cell* **79**, 315-328.

Parker, K. K., Brock, A. L., Brangwynne, C., Mannix, R. J., Wang, N., Ostuni, E., Geisse, N. A., Adams, J. C., Whitesides, G. M. and Ingber, D. E. (2002). Directional control of lamellipodia extension by constraining cell shape and orienting cell tractional forces. *FASEB J.* **16**, 1195-1204.

Plotnikov, S. V., Pasapera, A. M., Sabass, B. and Waterman, C. M. (2012). Force fluctuations within focal adhesions mediate ECM-rigidity sensing to guide directed cell migration. *Cell* **151**, 1513-1527.

Polacheck, W. J., German, A. E., Mammoto, A., Ingber, D. E. and Kamm, R. D. (2014). Mechanotransduction of fluid stresses governs 3D cell migration. *Proc. Natl. Acad. Sci. USA* [Epub ahead of print] doi: 10.1073/pnas.1316848111.

Salgia, R., Li, J. L., Ewaniuk, D. S., Wang, Y. B., Sattler, M., Chen, W. C., Richards, W., Pisick, E., Shapiro, G. I., Rollins, B. J. et al. (1999). Expression of the focal adhesion protein paxillin in lung cancer and its relation to cell motility. *Oncogene* **18**, 67-77.

Satchi-Fainaro, R., Mamluk, R., Wang, L., Short, S. M., Nagy, J. A., Feng, D., Dvorak, A. M., Dvorak, H. F., Puder, M., Mukhopadhyay, D. et al. (2005). Inhibition of vessel permeability by TNP-470 and its polymer conjugate, caplostatin. *Cancer Cell* **7**, 251-261.

Sawada, Y. and Sheetz, M. P. (2002). Force transduction by Triton cytoskeletons. *J. Cell Biol.* **156**, 609-615.

Sen, A., De Castro, I., Defranco, D. B., Deng, F. M., Melamed, J., Kapur, P., Raj, G. V., Rossi, R. and Hammes, S. R. (2012). Paxillin mediates extranuclear and intranuclear signaling in prostate cancer proliferation. *J. Clin. Invest.* **122**, 2469-2481.

Sero, J. E., Thodeti, C. K., Mammoto, A., Bakal, C., Thomas, S. and Ingber, D. E. (2011). Paxillin mediates sensing of physical cues and regulates directional cell motility by controlling lamellipodia positioning. *PLoS ONE* **6**, e28303.

Sero, J. E., German, A. E., Mammoto, A. and Ingber, D. E. (2012). Paxillin controls directional cell motility in response to physical cues. *Cell Adh. Migr.* **6**, 502-508.

Shen, J., Samul, R., Zimmer, J., Liu, H., Liang, X., Hackett, S. and Campochiaro, P. A. (2004). Deficiency of neuropilin 2 suppresses VEGF-induced retinal neovascularization. *Mol. Med.* **10**, 12-18.

Shimizu, A., Mammoto, A., Italiano, J. E., Jr, Pravda, E., Dudley, A. C., Ingber, D. E. and Klagsbrun, M. (2008). ABL2/ARG tyrosine kinase mediates SEMA3F-induced RhoA inactivation and cytoskeleton collapse in human glioma cells. *J. Biol. Chem.* **283**, 27230-27238.

Short, S. M., Yoder, B. J., Tarr, S. M., Prescott, N. L., Laniauskas, S., Coleman, K. A., Downs-Kelly, E., Pettay, J. D., Choueiri, T. K., Crowe, J. P. et al. (2007). The expression of the cytoskeletal focal adhesion protein paxillin in breast cancer correlates with HER2 overexpression and may help predict response to chemotherapy: a retrospective immunohistochemical study. *Breast J.* **13**, 130-139.

Tachibana, K., Sato, T., D'Avirro, N. and Morimoto, C. (1995). Direct association of pp125FAK with paxillin, the focal adhesion-targeting mechanism of pp125FAK. *J. Exp. Med.* **182**, 1089-1099.

Takashima, S., Kitakaze, M., Asakura, M., Asanuma, H., Sanada, S., Tashiro, F., Niwa, H., Miyazaki Ji, J., Hirota, S., Kitamura, Y. et al. (2002). Targeting of both mouse neuropilin-1 and neuropilin-2 genes severely impairs developmental yolk sac and embryonic angiogenesis. *Proc. Natl. Acad. Sci. USA* **99**, 3657-3662.

Tsubouchi, A., Sakakura, J., Yagi, R., Mazaki, Y., Schaefer, E., Yano, H. and Sabe, H. (2002). Localized suppression of RhoA activity by Tyr31/118-phosphorylated paxillin in cell adhesion and migration. *J. Cell Biol.* **159**, 673-683.

Turner, C. E., Glenney, J. R., Jr and Burridge, K. (1990). Paxillin: a new vinculin-binding protein present in focal adhesions. *J. Cell Biol.* **111**, 1059-1068.

Velasco-Velázquez, M. A., Salinas-Jazmín, N., Mendoza-Patiño, N. and Mandoki, J. J. (2008). Reduced paxillin expression contributes to the antimetastatic effect of 4-hydroxycoumarin on B16-F10 melanoma cells. *Cancer Cell Int.* **8**, 8.

Wacker, A. and Gerhardt, H. (2011). Endothelial development taking shape. *Curr. Opin. Cell Biol.* **23**, 676-685.

Wade, R., Bohl, J. and Vande Pol, S. (2002). Paxillin null embryonic stem cells are impaired in cell spreading and tyrosine phosphorylation of focal adhesion kinase. *Oncogene* **21**, 96-107.

Wild, J. R., Staton, C. A., Chapple, K. and Corfe, B. M. (2012). Neuropilins: expression and roles in the epithelium. *Int. J. Exp. Pathol.* **93**, 81-103.

Wozniak, M. A., Modzelewska, K., Kwong, L. and Keely, P. J. (2004). Focal adhesion regulation of cell behavior. *Biochim. Biophys. Acta* **1692**, 103-119.

Xia, N., Thodeti, C. K., Hunt, T. P., Xu, Q., Ho, M., Whitesides, G. M., Westervelt, R. and Ingber, D. E. (2008). Directional control of cell motility through focal adhesion positioning and spatial control of Rac activation. *FASEB J.* **22**, 1649-1659.

Yang, H. J., Chen, J. Z., Zhang, W. L. and Ding, Y. Q. (2010). Focal adhesion plaque associated cytoskeletons are involved in the invasion and metastasis of human colorectal carcinoma. *Cancer Invest.* **28**, 127-134.

Yano, H., Mazaki, Y., Kurokawa, K., Hanks, S. K., Matsuda, M. and Sabe, H. (2004). Roles played by a subset of integrin signaling molecules in cadherin-based cell-cell adhesion. *J. Cell Biol.* **166**, 283-295.

Yuan, L., Moyon, D., Pardanaud, L., Bréant, C., Karkkainen, M. J., Alitalo, K. and Eichmann, A. (2002). Abnormal lymphatic vessel development in neuropilin 2 mutant mice. *Development* **129**, 4797-4806.

Zaidel-Bar, R., Milo, R., Kam, Z. and Geiger, B. (2007). A paxillin tyrosine phosphorylation switch regulates the assembly and form of cell-matrix adhesions. *J. Cell Sci.* **120**, 137-148.

Fig. S1. Related to Figure 2. Paxillin knockdown controls vascular network formation in vivo. A) Schematic of Matrigel plug implant and experimental timeline. B) Graph showing endothelial cell migration into Matrigel implants treated with control or paxillin siRNA analyzed using immunohistochemical fluorescein-conA image analysis as measured in 3 random 50x50 μm fields per gel (n=4, **, $p<0.01$). C) Graph showing quantification of total cell migration into Matrigel implant treated with control or paxillin siRNA (n=7). D) Corresponding confocal micrographs to Fig. 2D, G of Matrigel implant treated with control or paxillin siRNA stained with DAPI. Scale bar; 50μm. E, F) Graphs showing number of CD45+ immune cells (E) and SMA+/CD31- fibroblasts (F) migrating into Matrigel implant treated with control or paxillin siRNA (n=4, *, $p<0.05$). Data are represented as mean +/- s.e.m.

Fig. S2. Related to Figures 4 and 7. Vinculin and zyxin knockdown do not affect NRP2 expression. A) Immunoblots showing paxillin, NRP2, vinculin, zyxin and GAPDH expression in HUVE cells treated with vinculin or zyxin siRNA. B) Graph showing mRNA levels of paxillin, NRP2, vinculin and zyxin in HUVE cells treated with vinculin or zyxin siRNA (***, $p<0.001$, *, $p<0.05$). C) Graph showing the number of migrating HUVE cells transfected with control, vinculin or zyxin siRNA normalized to control siRNA-transfected cells in Transwell migration assay. The migratory stimulus is 5% serum EGM2. D) Immunoblots showing NRP2 and GAPDH expression in HUVE cells treated with NRP2 siRNA or NRP2 DNA. E) Graph showing quantification of immunoblots of NRP2 in HUVE cells treated with NRP2 siRNA or DNA (***, $p<0.001$, *, $p<0.05$). F) Graph showing mRNA level of NRP2 in HUVE cells treated with NRP2 siRNA or DNA (**, $p<0.01$, *, $p<0.05$). G) Immunoblots showing GFP, NRP2 and GAPDH expression in HUVE cells transfected with paxillin siRNA with or without GFP-paxN or GFP-paxC DNA. H) Graph showing the number of migrating HUVE cells transfected with paxillin siRNA with or without GFP-paxN or GFP-paxC DNA normalized to paxillin siRNA-treated cells. (n=3, *, $p<0.05$). Data are represented as mean +/- s.e.m.

Fig. S3. Related to Figure 5. NRP2 knockdown controls vascular network formation in vivo. A) Confocal micrographs showing NRP2 expression (top) and DAPI (bottom) in control or NRP2 siRNA treated implants. Scale bar; 50μm. B) Graph showing NRP2 protein levels quantified via immunohistochemical image analysis where NRP2 colocalized to CD31+ cells as measured in 3 random 50x50 μm fields per gel (n=5, *, $p<0.05$). C) Graph showing mRNA level of NRP2 in the infiltrated cells in the implanted Matrigel (n=8, *, $p<0.05$). D) Quantification of total cell migration into Matrigel implant treated with control or NRP2 siRNA as measured in 3 random 50x50 μm fields per gel (n=4). E) Quantification of endothelial cell migration into Matrigel implant treated with control or NRP2 siRNA via immunohistochemical fluorescein-conA image analysis as measured in 3 random 50x50 μm fields per gel (n=3, **, $p<0.01$). F) Confocal micrographs showing VEGFR2 expression (top), CD31-stained blood vessels (bottom) in control or paxillin siRNA treated implants. Scale bar; 50μm. G) Quantification of VEGFR2 expression in Matrigel implant treated with control or paxillin siRNA via immunohistochemical analysis of VEGFR2 colocalized to CD31+ cells as measured in 3 random 50x50 μm fields per gel (n=4). H) Graph showing mRNA level of VEGFR2 in the infiltrated cells in the implanted Matrigel (n=8). Data are represented as mean +/- s.e.m.

Fig. S4. Related to Figure 6. LLC factors increase vascular network formation in vivo. A) Schematic of Matrigel plug implant (exploded view) and experimental timeline. B) H&E stained micrographs showing total cell migration from C57BL/6 mouse skin into implanted Matrigel with or without LLC factors. Scale bar; 50μm (top). Corresponding confocal micrographs to Fig. 6D showing CD31-stained

endothelial cells (middle) and DAPI stained nuclei (bottom) in the implanted Matrigel with or without LLC factors. Scale bar; 50µm. C) Quantification of vessel density in Matrigel implant with or without LLC factors via immunohistochemical CD31 image analysis as measured in 3 random 50x50um fields per tissue section (n=9, *, p<0.001). D) Graph showing migration distance of endothelial cells into Matrigel implant with or without LLC factors (n=7, *, p<0.001). E) Quantification of total cell migration into implant as measured in 3 random 50x50um fields per tissue section (n=4, *, p<0.001). F) Quantification of endothelial cell migration into Matrigel implant with or without LLC factors via immunohistochemical fluorescein-conA image analysis as measured in 3 random 50x50um fields per tissue section (n=4, *, p<0.001). Data are represented as mean +/- s.e.m.

Table S1. Target sequences for human and mouse siRNA.

Human paxillin #1 (target sequence is in paxillin C-terminus)	5’-GUGUGGAGCCUUCUUUGGU-3’
Human paxillin #2(target sequence is in paxillin N-terminus)	5'-CCACACAUACCAGGAGAUU-3'
Human NRP2	5’-CCAGAAGAUUGUCCUCAAC-3’
Human vinculin	5’-GGCAUAGAGGAAGCUUUAA-3’
Human zyxin	5’-CUGGACAUGGAGUUGGACCUGAGGC-3’
Mouse paxillin	5'-GAGCCCUCACCUACCGUCAU-3’
Mouse NRP2	5’-GAGCAGAGAGAAAGAAUAA-3’

Table S2. Sequences for primers for qRT-PCR.

	Forward	Reverse
Human paxillin	5’-CTGGCGGACTTGGAGTCTAC-3’	5’- CTCCTCCGACAAGAACACAGG-3’
Human NRP2	5’- CCAGAAGAUUGUCCUCAAC-3’	5’-GUUGAGGACAAUCUUCUGG-3’
Human vinculin	5’- CTCGTCCGGGTTGGAAAAGAG-3’	5’- AGTAAGGGTCTGACTGAAGCAT-3’
Human zyxin	5’-TCTCCCGCGATCTCCGTTT-3’	5’-CCGGAAGGGATTCACTTTGGG-3’
Human β2-micro-globulin	5’-GAATGGAGAGAGAATTGAAAAAGTGGAGCA-3’	5’-CAATCCAAATGCGGCATCTTCAAAC-3’
Mouse paxillin	5’-GGCATCCCAGAAAATAACACTCC-3’	5’- GCCCTGCATCTTGAAATCTGA-3’
Mouse NRP2	5’- GCTGGCTACATCACTTCCCC-3’	5’-CAATCCACTCACAGTTCTGGTG-3’
Mouse VEGFR2	5’-GCCCTGCCTGTGGTCTCACTAC-3’	5’-CAAAGCATTGCCCATTCGAT-3’
Mouse cyclophilin	5’-CAGACGCCACTGTCGCTTT-3’	5’-TGTCTTTGGAACTTTGTCTGCAA -3’

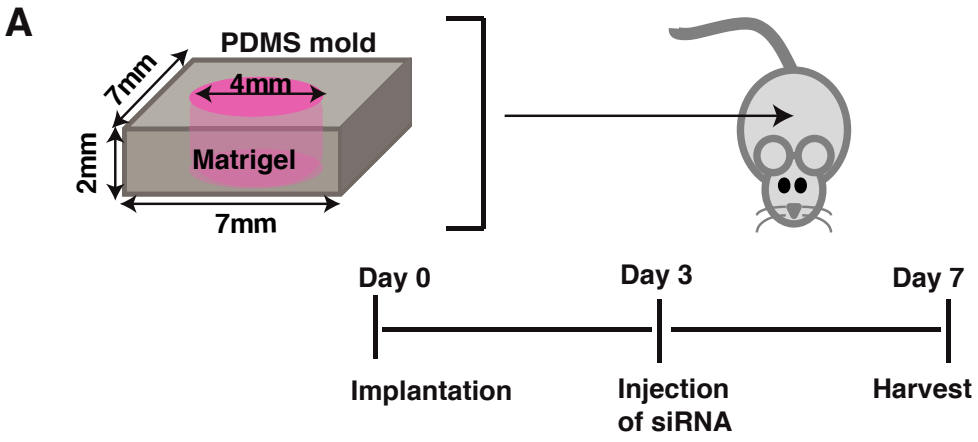

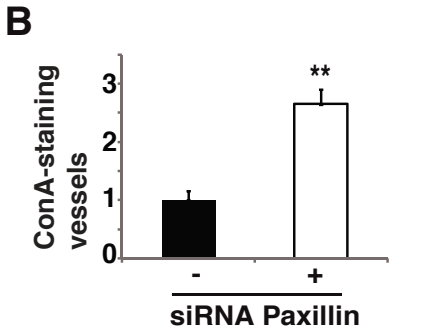

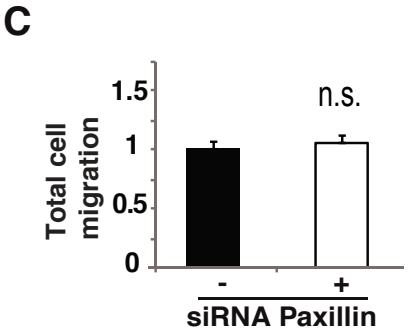

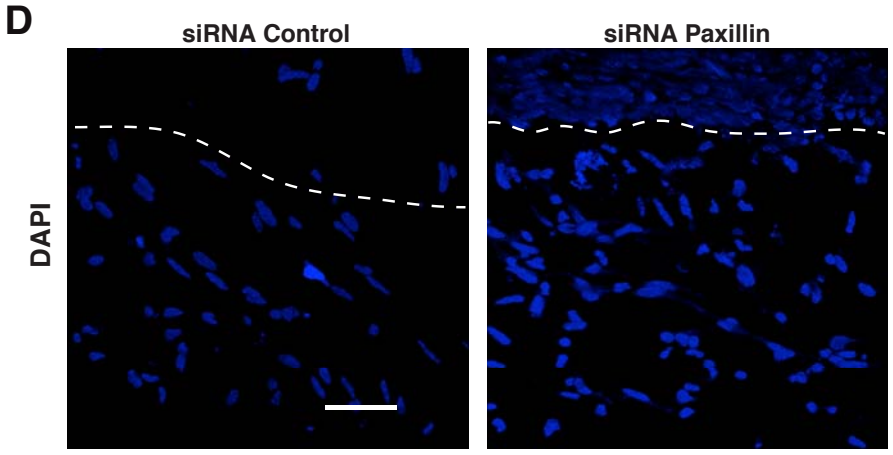

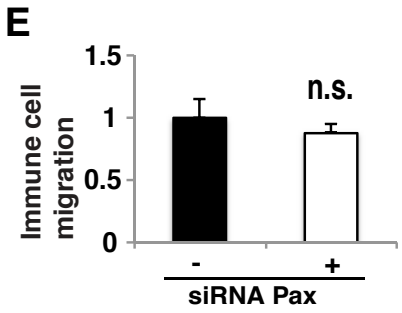

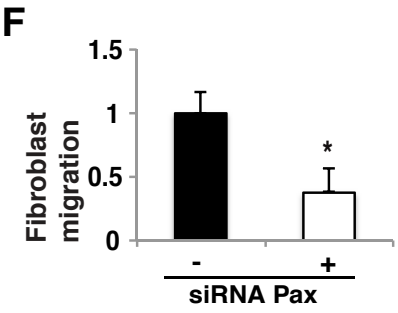

Supplementary Fig. S1

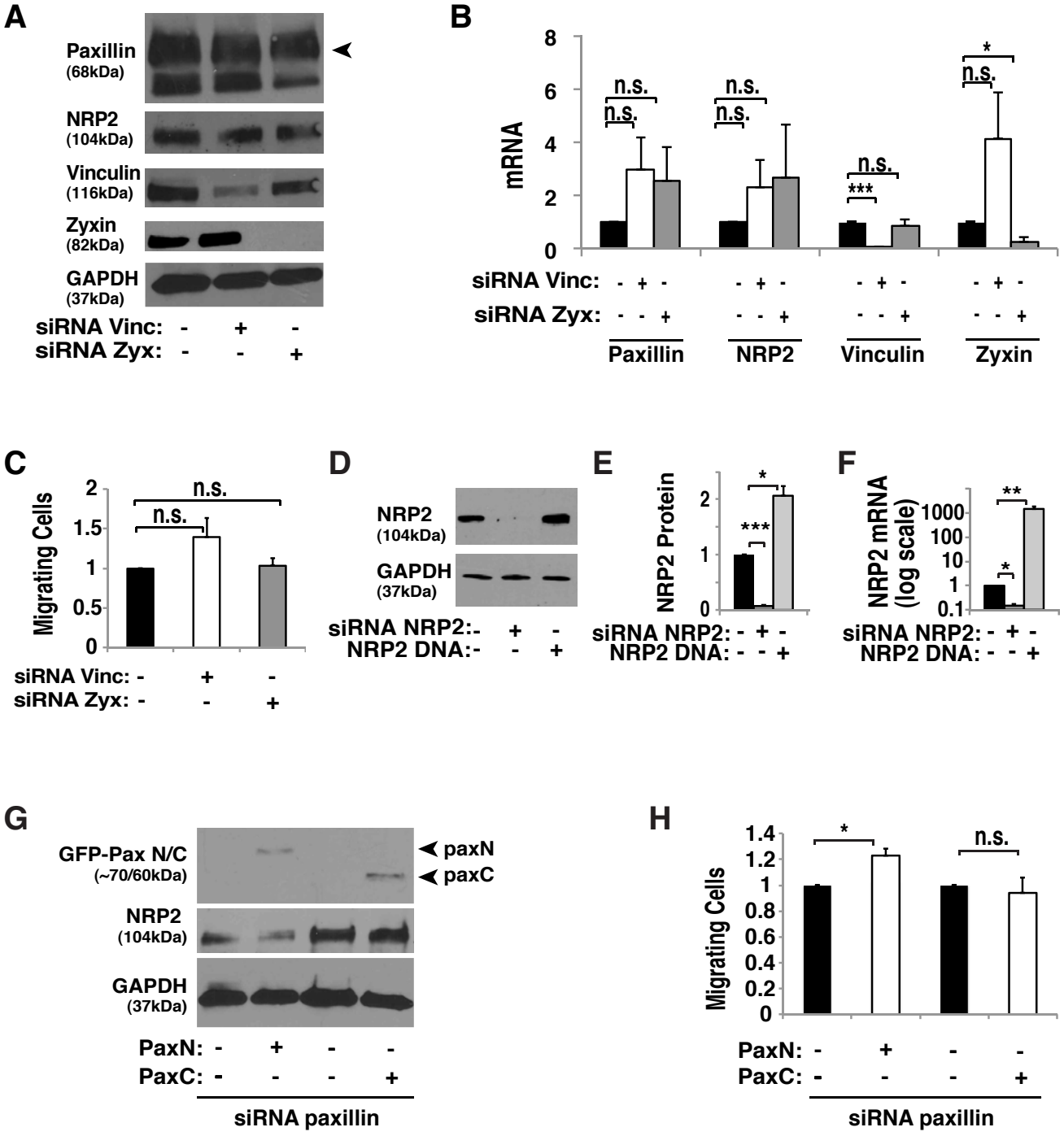

Supplementary Fig. S2

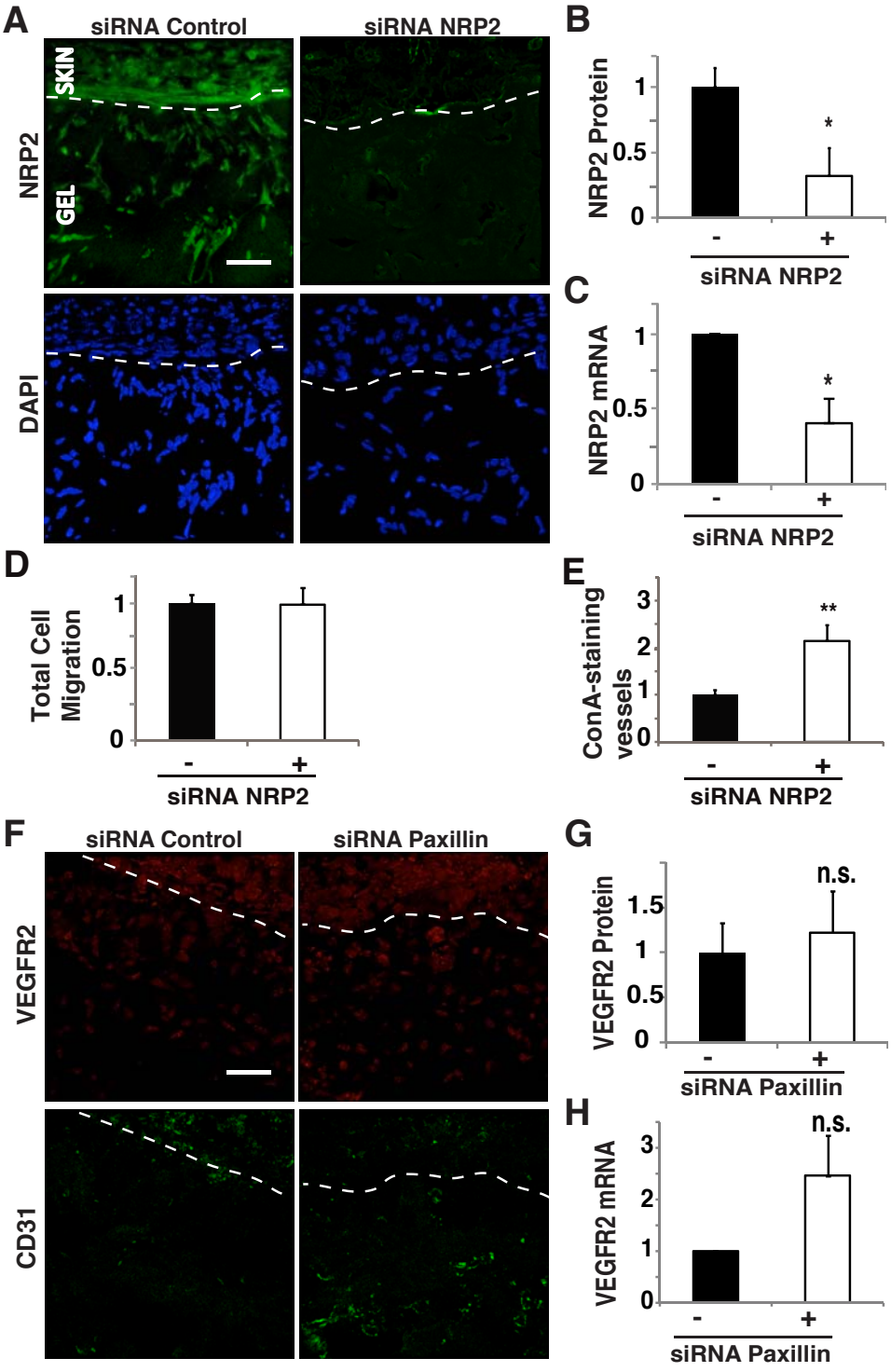

Supplementary Fig. S3

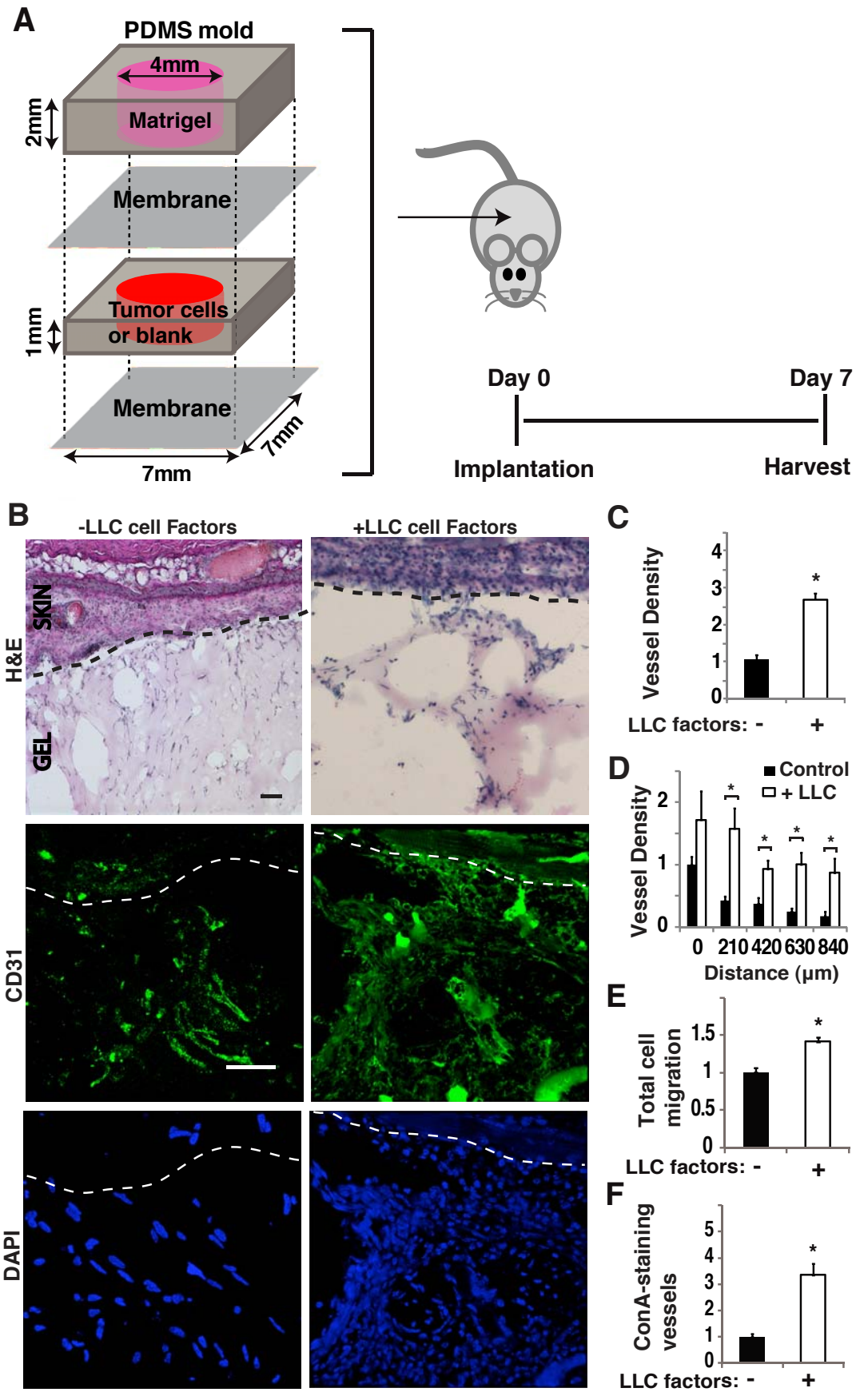

Supplementary Fig. S4